

# Identification of a Hormone-regulated Dynamic Nuclear Actin Network Associated with Estrogen Receptor $\alpha$ in Human Breast Cancer Cell Nuclei\*<sup>§</sup>

Concetta Ambrosino,<sup>a,b</sup> Roberta Tarallo,<sup>a</sup> Angela Bamundo,<sup>a</sup> Danila Cuomo,<sup>a</sup> Gianluigi Franci,<sup>a</sup> Giovanni Nassa,<sup>a</sup> Ornella Paris,<sup>a,c,d</sup> Maria Ravo,<sup>a</sup> Alfonso Giovane,<sup>e</sup> Nicola Zambrano,<sup>f</sup> Tatiana Lepikhova,<sup>g</sup> Olli A. Jänne,<sup>g</sup> Marc Baumann,<sup>h</sup> Tuula A. Nyman,<sup>i</sup> Luigi Cicatiello,<sup>a,c</sup> and Alessandro Weisz<sup>a,c,j,k</sup>

Estrogen receptor  $\alpha$  (ER $\alpha$ ) is a modular protein of the steroid/nuclear receptor family of transcriptional regulators that upon binding to the hormone undergoes structural changes, resulting in its nuclear translocation and docking to specific chromatin sites. In the nucleus, ER $\alpha$  assembles in multiprotein complexes that act as final effectors of estrogen signaling to the genome through chromatin remodeling and epigenetic modifications, leading to dynamic and coordinated regulation of hormone-responsive genes. Identification of the molecular partners of ER $\alpha$  and understanding their combinatorial interactions within functional complexes is a prerequisite to define the molecular basis of estrogen control of cell functions. To this end, affinity purification was applied to map and characterize the ER $\alpha$  interactome in hormone-responsive human breast cancer cell nuclei. MCF-7 cell clones expressing human ER $\alpha$  fused to a tandem affinity purification tag were generated and used to purify native nuclear ER-containing complexes by IgG-Sepharose affinity chromatography and glycerol gradient centrifugation. Purified complexes were analyzed by two-dimensional DIGE and mass spectrometry, leading to the identification of a ligand-dependent multiprotein complex comprising  $\beta$ -actin, myosins, and several proteins involved in actin filament organization and dynamics and/or known to participate in

actin-mediated regulation of gene transcription, chromatin dynamics, and ribosome biogenesis. Time course analyses indicated that complexes containing ER $\alpha$  and actin are assembled in the nucleus early after receptor activation by ligands, and gene knockdown experiments showed that gelsolin and the nuclear isoform of myosin 1c are key determinants for assembly and/or stability of these complexes. Based on these results, we propose that the actin network plays a role in nuclear ER $\alpha$  actions in breast cancer cells, including coordinated regulation of target gene activity, spatial and functional reorganization of chromatin, and ribosome biogenesis. *Molecular & Cellular Proteomics* 9:1352–1367, 2010.

Estrogens are potent tumor promoters for the mammary gland due to their growth-promoting actions in mammary epithelial cells (1). The mechanisms underlying stimulation of breast cell proliferation and control of the cell state by estrogens are still poorly defined despite the evident causal relationships between these hormonal actions and mammary gland carcinogenesis and cancer progression. Estrogen-responsive cells are endowed with specific estrogen receptors, ER $\alpha$ <sup>1</sup> and ER $\beta$ , members of the steroid/nuclear receptor superfamily of transcription factors that directly modulate the gene transcription rate (2). In addition, estrogens can trigger rapid and transient cellular responses through a mechanism(s) independent from this “genomic” pathway of steroid receptor action (3, 4). Such “extragenomic” effects include cell type-specific, rapid, and transient responses of signal transduction pathways; induction of intracellular calcium mobilization; and

From the Departments of <sup>a</sup>General Pathology and <sup>b</sup>Biochemistry and Biophysics “F. Cedrangolo,” Second University of Naples, 80138 Naples, Italy, <sup>c</sup>Department of Biological and Environmental Sciences, University of Sannio, 82100 Benevento, Italy, <sup>d</sup>Associazione Italiana per la Ricerca sul Cancro (AIRC) Naples Oncogenomics Center, 80145 Naples, Italy, <sup>e</sup>CEINGE Biotechnologie Avanzate and Department of Biochemistry and Medical Biotechnologies, University of Naples Federico II, 80145 Naples, Italy, <sup>f</sup>Institute of Biomedicine (Physiology) and <sup>g</sup>Protein Chemistry Unit, Biomedicum Helsinki, University of Helsinki, 00290 Helsinki, Finland, <sup>h</sup>Protein Chemistry Research Group, Institute of Biotechnology, University of Helsinki, 00790 Helsinki, Finland, and <sup>i</sup>Molecular Medicine Laboratory, Faculty of Medicine and Surgery, University of Salerno, 84081 Baronissi, Italy

Received, November 2, 2009, and in revised form, February 22, 2010

Published, MCP Papers in Press, March 22, 2010, DOI 10.1074/mcp.M900519-MCP200

<sup>1</sup> The abbreviations used are: ER, estrogen receptor; aa, amino acid; Ab, antibody; ChIP, chromatin immunoprecipitation; Cyt D, cytochalasin D; E<sub>2</sub>, 17 $\beta$ -estradiol; ERE, estrogen response element; *kd*, protein expression “knockdown” by shRNA; RNP, ribonucleoparticle; Tam, 4-hydroxytamoxifen; TAP, tandem affinity purification; TEV, tobacco etch virus; WB, Western blotting; BC, breast cancer; UniHI, Unified Human Interactome; shRNA, short hairpin RNA; GSN, gelsolin; FLII, flightless I; MYO, myosin 1c; wt, wild type; G, globular; F, filamentous; EtOH, ethanol.

activation of membrane ion channels. The genomic and extragenomic pathways do integrate with each other to mediate the mitogenic actions of estrogen, including activation of cell cycle-controlling gene networks (5). Both of these cascades involve multiple molecular components that modulate and/or mediate ER activity by functionally or physically interacting with them in specific cellular compartments, such as plasma membrane (6, 7), cytoplasm, and chromatin (8–10). Indeed, it is well known that most effects of estrogens are cell type-specific (3, 11–14), and this is achieved by differential expression of not only ERs but also functional partners of these receptors. These are believed to include transcriptional co-regulators, signaling effectors, molecular adapters, and other intracellular molecules (15–18), which participate in estrogen signal transduction within modular multiprotein complexes with different biological activities depending upon their absolute composition, stoichiometry, and conformation of their components (19–21). Understanding the nature of the cellular proteins acting in concert with ERs to control cell functions is an open issue in breast cancer biology (22–27). To date, this issue has been addressed by analysis of molecular profiles associated with hormone response and disease state in breast cancer cells. Gene expression profiling (28–30) and quantitative proteomics analyses (31, 32) provided a blueprint of the effects of estrogen and other ER ligands in hormone-responsive cancer cells, revealing a complexity of ER-induced cellular responses that suggests the likelihood that ERs exist in the cell in multiple functional conformations. Indeed, the already mentioned ability of ligand-activated ERs to form multiple complexes with key intracellular regulatory molecules represents a well known mechanism to explain their multifaceted effects in key processes such as signal transduction and transcriptional regulation (2, 6). For this reason, we established an experimental model to identify and characterize the nuclear ER interactome of hormone-responsive human breast cancer cells. We focused on ER $\alpha$ , the main mediator of estrogen action in breast cancer cell nuclei, and established an experimental procedure to purify native ER-containing multi-molecular complexes from estrogen-treated cell nuclei by affinity chromatography. ER $\alpha$  fused to a tandem affinity purification (TAP) tag was stably expressed in MCF-7 cells. By combining one-step (IgG-Sepharose) affinity purification and glycerol gradient centrifugation, we isolated ER-containing native complexes that were then analyzed by two-dimensional DIGE and/or mass spectrometry. In this way, we identified nuclear  $\beta$ -actin and several actin-binding proteins bound to ER $\alpha$  in BC cell nuclei following hormonal stimulation. It has been recently demonstrated that  $\beta$ -actin and its binding partners are important regulators of several nuclear processes, including all transcriptional steps and chromatin remodeling (33–36), repositioning of actively transcribed genes to the periphery of nuclear territories (37), and enhancer-promoter interactions by intra- and interchromosomal looping (9). These findings, combined with the identification of the

same proteins in stable ER $\alpha$  complexes within the nucleus, indicate that the nuclear  $\beta$ -actin pathway is part of the molecular machinery that allows control of genome activity and structural organization by estrogen via ER $\alpha$ .

#### EXPERIMENTAL PROCEDURES

**Cell Lines and Plasmid Preparation**—The following human breast cancer cell lines were used: ER $\alpha$ -positive MCF-7 and MELN cells, the latter derived from MCF-7 cells and carrying the luciferase gene under the control of an 17 $\beta$ -estradiol (E $_2$ )-regulated promoter stably integrated in the genome (38), and ER $\alpha$ -negative MDA-MB-231 cells. MCF-7 Tet-Off cells (Clontech) were used to generate stable clones. All cell lines were cultured in Dulbecco's modified Eagle's medium (Sigma-Aldrich) and 10% FCS (HyClone) supplied with 100 units/ml penicillin, 100 mg/ml streptomycin, 250 ng/ml amphotericin B, and 50  $\mu$ g/ml G418 (standard growth conditions). E $_2$ -deprived cells (starved cells) were obtained by culturing in Dulbecco's modified Eagle's medium without phenol red and 5% steroid-deprived serum (dextran-coated charcoal-treated FCS) for 5 days as described earlier (39).

The TAP tag fragment of 500 bp was contained in the expression vector pZOME 1-C (CellZome) kindly provided by Dr. G. Superti-Furga. This fragment, obtained after enzymatic digestion with EcoRI and BamHI, was subcloned into the pUSE amp(+) vector (Upstate). pUSE-C-TAP resulted from this subcloning. The full-length coding region of the human ER $\alpha$  cDNA was PCR-amplified, creating a BamHI site prior to the ATG codon to obtain the plasmid pUSE-C-TAP-ER $\alpha$ . The cDNA sequence encoding C-TAP-ER $\alpha$  was then subcloned in the mammalian tetracycline-inducible expression vector pTRE2purHA cut with EcoRV and BamHI to generate pTRE2purHA-C-TAP-ER $\alpha$ .

For generation of FLAG-ER $\alpha$ , the cDNA sequence encoding human ER $\alpha$  was cloned in the mammalian expression vector p3XFLAG-CMV (Sigma-Aldrich) after digestion with the restriction enzyme BamHI to obtain p3XFLAG-CMV-ER $\alpha$ . The expression vector pEF-FLAG-actin encoding N-FLAG- $\beta$ -actin (40) was kindly provided by Dr. G. Posern.

**Transient Transfection and Luciferase Assay**—For transient transfection, cells (MDA-MB-231 or MCF-7) were seeded ( $5 \times 10^5$  cells/60-mm dish) either in standard growth medium or in starvation medium and transfected by using Lipofectamine 2000 reagent (Invitrogen) according to the manufacturer's instructions using 3.5  $\mu$ g/dish DNA. The transfection mixture was removed after 6 h, and cells were treated as indicated and lysed 24 h later. Ratios between the number of plated cells, plate size, and amount of DNA-liposome complexes were kept constant in all cases.

For luciferase reporter-gene assays, cells were plated in E $_2$ -deprived medium and transfected as described above with 3.5  $\mu$ g of DNA including 300 ng of ERE-TK-luc, 500 ng of pSG $\Delta$ 2-NLS-LacZ, 2600 ng of BlueScribe M13+, and 100 ng of ER $\alpha$  or TAP-ER $\alpha$  expression vectors or, alternatively, the corresponding "empty" expression vector as described previously (41). Six hours after transfection, the medium was changed, and 24 h later cells were stimulated with  $10^{-8}$  M E $_2$ . After 24 h, cells were harvested, and the luciferase activity was measured using the Luciferase Assay Reagent (Promega Corp.) according to the manufacturer's instructions, and values were expressed as relative light units normalized to the  $\beta$ -galactosidase activity or to the protein concentrations measured using the Bradford assay. For each condition, average luciferase activity was calculated from the data obtained from three independent dishes and three independent experiments.

**Stable Transfection Procedure**—MCF-7 Tet-Off cells ( $6-7 \times 10^5$ /60-mm dish) were plated and transfected with 3.5  $\mu$ g of pTRE2purHA-C-TAP (empty vector, TAP) or pTRE2purHA-C-TAP-ER $\alpha$  (TAP-ER $\alpha$ ) as described above. After 48 h, cells were transferred to 150-mm dishes, and the selection was carried out in the presence of

50  $\mu$ g/ml G418, 0.5  $\mu$ g/ml doxycycline, and 0.5  $\mu$ g/ml puromycin. Resistant clones were picked up after 2–3 weeks, expanded separately, and screened by immunoblotting. Expression of the exogenous protein was constitutive in most cases (doxycycline-independent; data not shown).

**Western Blotting and Antibodies**—Protein samples were separated by electrophoresis as described earlier (39) using homogeneous gels containing 7, 8, or 10% polyacrylamide and 0.1% SDS (SDS-PAGE) and transferred to nitrocellulose membranes (Whatman GmbH). Membranes were blocked with 5% nonfat dry milk in TBST buffer (0.01 M Tris-HCl, pH 8.0, 0.15 M NaCl, and 0.1% Tween 20) and incubated with the following Abs: rabbit polyclonal anti-ER $\alpha$  (sc-543), -Arp2 (sc-15389), -Arp3 (sc-15390), and -lamin B (sc-6216) from Santa Cruz Biotechnology; mouse monoclonal anti- $\beta$ -actin (A1978) and - $\alpha$ -tubulin (T6199), rabbit polyclonal anti-myosin 1c (nuclear isoform, M3567), and mouse monoclonal anti-FLAG M2 (F1804) from Sigma-Aldrich; rabbit polyclonal anti-TAP (CAB1001) from Open Biosystems; mouse monoclonal anti-flightless I (ab28089) and -gelsolin (ab11081), rabbit monoclonal anti-nucleophosmin (ab52644), and rabbit polyclonal anti-DDX5 (ab21696) from Abcam; and mouse monoclonal anti-RNA polymerase II (MMS-126R) from Covance. Each Ab was used according to the manufacturer's protocols. After extensively washing with TBST, the primary Abs were detected by the appropriate horseradish peroxidase-conjugated secondary Abs (GE Healthcare) and revealed by chemiluminescence and autoradiography.

**Cell Cycle Analysis**—Cells ( $1.5 \times 10^5$  cells/60-mm dish) were starved for 5 days and subsequently stimulated with  $10^{-8}$  M E $_2$ . G $_1$ -to-S transition kinetics were first determined in hormone-stimulated MCF-7 Tet-Off cells (supplemental Fig. S1). This showed that 27 h into hormonal stimulation was the optimal timing to measure the mitogenic effect of the hormone as >50% cells are in S and G $_2$ /M phases at this time, confirming our previous observations (29, 30, 41). To study cell cycle progression, TAP- and TAP-ER $\alpha$ -expressing cells were thus collected 27 h after E $_2$  addition in PBS containing 50  $\mu$ g/ml propidium iodide, 0.1% (v/v) sodium citrate, and 0.1% (v/v) Nonidet P-40 and analyzed with a FACScalibur flow cytometer using the CellQuest software package (BD Biosciences). Data analysis was performed with Modfit software (Verity Software). Values were plotted as increasing numbers of S + G $_2$  phase cells with respect to non-stimulated controls. Results were obtained from several independent experiments.

**Preparation of Nuclear Extracts**—Cells were harvested by scraping in cold PBS, collected by centrifugation at  $1000 \times g$ , and resuspended in 3 volumes with respect to the cell pellet of hypotonic buffer (20 mM HEPES, pH 7.4, 5 mM NaF, 10  $\mu$ M sodium molybdate, 0.1 mM EDTA, 1 mM DTT, 1 mM PMSF, and  $1 \times$  protease inhibitor mixture (Sigma-Aldrich)). Upon incubation on ice for 15 min, 0.5% Triton X-100 was added, and a cytosolic fraction was prepared by spinning the samples for 30 s at 4  $^{\circ}$ C at  $15,000 \times g$  and subsequently clarified by centrifugation ( $15,000 \times g$  for 15 min at 4  $^{\circ}$ C). The nuclear pellets were first washed twice in hypotonic buffer to remove any residual cytosolic contaminations and then resuspended in 1 volume of nuclear lysis buffer (20 mM HEPES, pH 7.4, 25% glycerol, 420 mM NaCl, 1.5 mM MgCl $_2$ , 0.2 mM EDTA, 1 mM DTT,  $1 \times$  Sigma-Aldrich protease inhibitor mixture, and 1 mM PMSF), incubated for 30 min at 4  $^{\circ}$ C with gentle shaking, and finally centrifuged for 30 min at 4  $^{\circ}$ C at  $15,000 \times g$ . The nuclear pellets were examined microscopically to control for the presence of residual intact cells, and the nuclear extracts were assayed in all cases by Western blotting with antibodies against nuclear (lamin B) and cytoplasmic ( $\alpha$ -tubulin) protein markers. No significant cross-contamination between the two cellular compartments could be detected (see a representative test in supplemental Fig. S2).

**TAP Procedure**—TAP- and TAP-ER $\alpha$ -expressing cells ( $6 \times 10^8$ – $10^9$  cells in 500-cm $^2$  plates) were starved and stimulated with  $10^{-8}$  M E $_2$  for 2h. Cells were collected, extensively washed with ice-cold PBS, and lysed as described above. Nuclear or, where indicated, cytoplasmic extracts were diluted with a  $2 \times$  volume of nuclear lysis buffer without NaCl and incubated with 6  $\mu$ l/mg protein IgG-Sepharose beads (IgG-Sepharose 6 Fast Flow, GE Healthcare). Before incubation, the beads were treated according to the manufacturer's instructions, equilibrated in 10 volumes of TEV buffer (50 mM Tris-HCl, pH 8.0, 0.5 mM EDTA, 1 mM DTT, 0.1% Triton X-100, and 150 mM NaCl), and washed four times with 20 volumes of IPP150 buffer (20 mM HEPES, pH 7.5, 8% glycerol, 150 mM NaCl, 0.5 mM MgCl $_2$ , 0.1 mM EDTA, and 0.1% Triton X-100) at 4  $^{\circ}$ C for 15 min. The beads were then added to the samples, and binding was performed for 4 h at 4  $^{\circ}$ C on a rotating platform. At the end, the unbound proteins were collected by centrifugation, and the beads were washed with 100 volumes of IPP150 and 30 volumes of TEV buffer in a Poly-Prep chromatography column (0.8  $\times$  4 cm, Bio-Rad) at 4  $^{\circ}$ C. Finally, 4 bead volumes of TEV buffer containing 1 unit of TEV protease/ $\mu$ l of beads (Invitrogen) were added, and following incubation for 2 h at 16  $^{\circ}$ C on a shaking platform (Thermomixer, Eppendorf), the released proteins were collected by centrifugation.

**Two-dimensional DIGE and Protein Identification by LC-MS/MS**—Two-dimensional DIGE was performed on TEV eluates prepared from TAP and TAP-ER $\alpha$  purified samples concentrated by precipitation with TCA/acetone. After washing with ice-cold acetone, the sample pellets were dried and resuspended in buffer containing 7 M urea, 2 M thiourea, 4% (w/v) CHAPS, and 30 mM Tris-HCl, pH 8.5. The samples were separately labeled with cyanine dyes (Cy2 and Cy3 for TAP and TAP-ER $\alpha$  samples, respectively), and after incubation on ice for 30 min in the dark, the labeling reaction was stopped by adding 10 mM L-lysine and incubation for 15 min. Proteins from each sample were mixed with rehydration buffer (30 mM Tris-HCl, pH 8.5, 7 M urea, 2 M thiourea, 4% (w/v) CHAPS, 2% (w/v) DTT, IPG Buffer, pH 3–10 non-linear for IEF, 1.4% (v/v) DeStreak solution, and bromphenol blue) and loaded on an Immobiline DryStrip (24 cm, pH 3–10 non-linear from GE Healthcare). After rehydration overnight, strips were focused (IPGphor II, GE Healthcare). Once IEF was complete, the strips were equilibrated in 100 mM Tris, pH 8.0, 6 M urea, 30% (v/v) glycerol, 2% (w/v) SDS, and bromphenol blue with addition of 0.5% (w/v) DTT for 15 min followed by the same buffer without DTT but with the addition of 4.5% (w/v) iodoacetamide (Sigma-Aldrich) for 15 min. SDS-PAGE was performed on a 12% polyacrylamide gel without a stacking gel using the Ettan DALTsix system (GE Healthcare). After the second dimension, fluorescent images were acquired using the Typhoon 9400 laser scanner (GE Healthcare) and subsequently analyzed with the Differential In-gel Analysis (DIA) module of the DeCyder software package (GE Healthcare) after staining with SYPRO Ruby (Invitrogen) according to the manufacturer's instructions.

The specific spots detected in the TAP-ER $\alpha$  sample were selected, excised from the gel, and washed in 50 mM ammonium bicarbonate, pH 8.0 in 50% acetonitrile for a complete destaining. The gel slices were resuspended in 50 mM ammonium bicarbonate, pH 8.0 containing 100 ng of trypsin and incubated for 2 h at 4  $^{\circ}$ C and overnight at 37  $^{\circ}$ C. The supernatant containing the resulting peptide mixtures was removed, and the gel pieces were re-extracted with acetonitrile. The two fractions were then collected, pooled, and freeze-dried.

The peptide mixtures were analyzed by LC-MS/MS using an LC/MSD Trap XCT Ultra instrument (Agilent Technologies) equipped with an 1100 HPLC system and a chip cube (Agilent Technologies). After loading, the peptide mixture (7  $\mu$ l in 0.5% TFA) was first concentrated at 4  $\mu$ l/min in a 40-nl enrichment column (Agilent Technologies) with 0.1% formic acid as eluent. The sample was then fractionated on a C $_{18}$  reverse-phase capillary column (75  $\times$  43 mm, Agilent Technolo-

gies) at a flow rate of 300 nl/min with a linear gradient of eluent B (0.1% formic acid in acetonitrile) in eluent A (0.1% formic acid) from 7 to 50% in 35 min. Elution was monitored on the mass spectrometers without any splitting device. Peptide analysis was performed with MSD TRAP CONTROL 6.0 (Agilent Technologies) using data-dependent acquisition of one MS scan ( $m/z$  range from 400 to 2000 Da/e) followed by MS/MS scans of the three most abundant ions in each MS scan. Dynamic exclusion was used to acquire a more complete survey of the peptides by automatic recognition and temporary exclusion (2 min) of ions from which definitive mass spectral data had previously been acquired. Moreover, a permanent exclusion list of the most frequent peptide contaminants (keratins and trypsin peptides) was included in the acquisition method to focus the analyses on significant data.

Mass spectral data obtained from the LC-MS/MS analyses were used to search a non-redundant protein database (NCBI nr, January 22, 2007; 4,473,090 sequences; 1,537,870,565 residues; taxonomy, *Homo sapiens* (human): 190,985 sequences) using an in-house version of the Mascot software (version 2.1; Matrix Science). Peptide mass values and sequence information from LC-MS/MS experiments were used in the MS/MS ion search taking into account carbamidomethyl-Cys as a fixed modification and precursor ion and fragment ion mass tolerances of  $\pm 600$  ppm and 0.6 Da, respectively. All of the reported protein identifications were statistically significant ( $p < 0.05$ ).

**Nano-LC-MS/MS Analysis**—Purified protein complexes eluted by TEV protease digestion were precipitated by TCA/acetone. Pellets were washed with ice-cold acetone, dried, resuspended in 0.1 M NaH<sub>4</sub>HCO<sub>3</sub> and 10% acetonitrile (HPLC grade S, Rathburn Chemicals), sonicated, and dried again to the optimal volume. Then, sequencing grade modified trypsin (Promega Corp.) was added to the samples, which were digested overnight at 37 °C with gentle agitation. The resulting peptides were dissolved in 0.1% TFA and analyzed by LC-MS/MS using an UltiMate 3000 nano-LC system (Dionex) and a QSTAR Elite hybrid quadrupole TOF-MS instrument (Applied Biosystems/MDS Sciex) with nano-ESI. The LC-MS/MS samples were first loaded on a ProteoCol C<sub>18</sub> trap column (10 mm  $\times$  150  $\mu$ m, 3  $\mu$ m, 120 Å) (SGE Analytical Science) followed by peptide separation on a PepMap100 C<sub>18</sub> analytical column (15 cm  $\times$  75  $\mu$ m, 5  $\mu$ m, 100 Å) (LC Packings/Dionex) at 200 nl/min. The separation gradient consisted of 0–50% B in 50 min, 50% B for 3 min, 50–100% B in 2 min, and 100% B for 3 min (buffer A, 0.1% formic acid; buffer B, 0.08% formic acid in 80% acetonitrile). MS data were acquired using Analyst QS 2.0 software. The information-dependent acquisition method consisted of a 0.5-s TOF-MS survey scan of  $m/z$  400–1400. From every survey scan, the two most abundant ions with charge states 2+ to 4+ were selected for product ion scans. Once an ion was selected for MS/MS fragmentation, it was put on an exclusion list for 60 s.

The LC-MS/MS data were searched in Swiss-Prot 57.0 (428,650 sequences; 154,416,236 residues; taxonomy, *H. sapiens* (human): 20,334 sequences) with the in-house Mascot version 2.2 through the ProteinPilot 2.0.1 interface against the Swiss-Prot database (version 57.0). The criteria for Mascot searches were as follows: human-specific taxonomy, trypsin digestion with one missed cleavage allowed, and oxidation of methionine as a variable modification. For the LC-MS/MS spectra, the maximum precursor ion mass tolerance was 50 ppm and MS/MS fragment ion mass tolerance was 0.2 Da, and a peptide charge state of 1+, 2+, or 3+ was used. All of the reported protein identifications were statistically significant ( $p < 0.05$ ). To eliminate the redundancy of proteins that appear in the database under different names and accession numbers, the single protein member with the highest protein score (top rank) was selected from multiprotein families for the identification results. To perform the protein networking analysis, the list of proteins identified by nano-LC-MS/MS was crossed with the list containing only direct  $\beta$ -actin inter-

actors from the UniProt database (42), and the results were visualized with the UniProt search visualization tool options.

**Protein Complex Immunoprecipitation**—FLAG-actin and FLAG-ER $\alpha$  were immunoprecipitated by incubation of nuclear extracts from transiently transfected MCF-7 cells with anti-FLAG M2-agarose (Sigma-Aldrich) for 2 h at 4 °C. After extensively washing, immunoprecipitated proteins were eluted under native condition by a competition with 3 $\times$  FLAG peptide (Sigma-Aldrich).

For immunoprecipitation of endogenous ER $\alpha$ , nuclear extracts from MCF-7 cells (500  $\mu$ g) were precleared with normal rabbit IgG (Santa Cruz Biotechnology) and protein G-Sepharose (protein G-Sepharose 4 Fast Flow, GE Healthcare) for 30 min. After preclearing, 2  $\mu$ g of specific Ab were added and incubated for 2 h at 4 °C while rotating, and then protein G-Sepharose was added for 1 h. Immunoprecipitated proteins were collected by centrifugation, and after washing, the beads were resuspended in Laemmli buffer. Control immunoprecipitations were performed by using anti-green fluorescent protein antibodies (sc-8334, Santa Cruz Biotechnology).

**Chromatin Immunoprecipitation (ChIP)**—Chromatin was isolated and immunoprecipitated with minor modifications as described earlier (41).  $5 \times 10^6$  cells were fixed in 1% formaldehyde for 10 min at room temperature, and the reaction was stopped by adding glycine at a final concentration of 0.125 M. Upon washing with ice-cold PBS, the cells were harvested by scraping, pelleted, and resuspended in SDS lysis buffer. Samples were sonicated with a Bioruptor sonicator (Diagenode) for 12  $\times$  30-s cycles at high power, centrifuged at 15,000  $\times$  g for 15 min, and diluted 8-fold in ChIP dilution buffer. After removing an aliquot for further use (input), samples were incubated at 4 °C overnight with Abs against ER $\alpha$  or  $\beta$ -actin. Complexes were precipitated with protein A-agarose/salmon sperm DNA beads and washed sequentially with low salt immune complex washing buffer, high salt immune complex wash buffer, LiCl immune complex washing buffer, and Tris-EDTA buffer twice. Immunoprecipitated chromatin was eluted in elution buffer, incubated at 65 °C overnight, and treated with proteinase K. DNA was purified by extracting with phenol/chloroform/isoamyl alcohol (25:24:1) and precipitating in ethanol. DNA pellets were resuspended in nuclease-free water and analyzed by real time PCR carried out using Power SYBR Green PCR Master Mix (Applied Biosystems) in an MJ Research PTC-200 Opticon instrument with the following primers for pS2/TFF1 gene promoter: forward, ctgacgggaatgggctcat; reverse, gcttgccctgacaacagtg. -Fold enrichment was determined using 2  $\mu$ l of input DNA as template and was determined in independently replicated ChIP assays.

**G-actin/F-actin Assay and Glycerol Gradient Centrifugation Analysis**—The G-actin/F-actin assay kit was purchased from Cytoskeleton Inc. (BK037), and the assessment of ER $\alpha$  association to globular or filamentous actin after E<sub>2</sub> stimulation was performed according to the manufacturer's instructions and previously published studies (43, 44).

For fractionation of protein complexes, nuclear extracts or TEV eluates were layered over a discontinuous density gradient comprising nine steps of 5–45% glycerol in TEV buffer. The samples were centrifuged at 29,000 rpm (TST41.14 rotor, Kontron) for 18 h. At the end of the run, 20 fractions of 500  $\mu$ l each were collected stepwise from the top of the gradient, and the bottom fraction was recovered by gently washing the tube with TEV buffer. The fractions were either directly analyzed by immunoblotting or precipitated by adding 1 volume of acetone/TCA (9:1) and incubating the mixture overnight at –20 °C. The precipitated samples were centrifuged at 13,000  $\times$  g for 90 min, washed with ice-cold acetone, dried, and resuspended in Laemmli buffer. After denaturation, the samples were analyzed by SDS-PAGE and WB. Insulin (3.1 S), aldolase (7.3 S), catalase (11.4 S), and ferritin (18.0 S) were used as sedimentation markers. Their position in the gradient was revealed by the Bradford assay.

**Lentiviral Transduction**—Lentiviral knockdown was performed using pLKO.1 plasmid vectors (Sigma-Aldrich) expressing shRNAs targeting the gelsolin (GSN) (GenBank™ accession number NM\_000177), flightless I (FLII) (GenBank accession number NM\_002018), or MYO1C (GenBank accession number NM\_033375) transcripts in different regions. Lentivirus production was performed by co-transfecting 293FT cells (Invitrogen) with shRNA vector and packaging plasmids using Lipofectamine 2000 (Invitrogen). The viral particles obtained were then used to transduce MCF-7 cells. Duplicates of  $3.5 \times 10^5$  cells were plated in 6-well plates and 24 h later infected by adding lentiviral particles and Polybrene at a final concentration of 8  $\mu$ g/ml. The transduction medium was replaced with fresh culturing medium 6 h after infection. Transduced cells were selected by adding puromycin at a final concentration of 1  $\mu$ g/ml for 10 days. Western blotting and quantitative RT-PCR were performed to screen the cell pools obtained for effective depletion of the target protein and mRNA, respectively. Stable cell clones were obtained with the following shRNA-expressing lentiviruses from Sigma-Aldrich: TRCN0000029726 (GSN<sub>(1)</sub>), TRCN0000029728 (GSN<sub>(2)</sub>), TRCN0000029724 (GSN<sub>(3)</sub>), TRCN0000029727 (GSN<sub>(4)</sub>), and TRCN0000029725 (GSN<sub>(5)</sub>) targeting gelsolin; TRCN0000157051 (FLII<sub>(1)</sub>), TRCN0000152827 (FLII<sub>(2)</sub>), TRCN0000157237 (FLII<sub>(3)</sub>), TRCN0000152063 (FLII<sub>(4)</sub>), and TRCN0000157412 (FLII<sub>(5)</sub>) targeting flightless I; and TRCN0000122924 (MYO<sub>(1)</sub>), TRCN0000122926 (MYO<sub>(2)</sub>), TRCN0000122927 (MYO<sub>(3)</sub>), and TRCN0000122928 (MYO<sub>(4)</sub>) targeting myosin 1c. Only the GSN<sub>(1)</sub>, GSN<sub>(2)</sub>, FLII<sub>(3)</sub>, MYO<sub>(1)</sub>, and MYO<sub>(2)</sub> clones showed a significant reduction of the targeted protein levels and were used for the tests described.

RESULTS

**Characterization and Stable Expression of TAP-ER $\alpha$  Fusion Protein in MCF-7 Cells**—To generate a suitable fusion protein for TAP (45), the human ER $\alpha$  coding sequence was cloned upstream of a TAP tag comprising the IgG binding domain of protein A and a calmodulin binding peptide separated by a peptide carrying a TEV protease cleavage site (Fig. 1A) to generate TAP-ER $\alpha$ . Several experiments were then performed to test TAP-ER $\alpha$  functionality in breast cancer cells. First, we controlled whether tagging interfered with ER $\alpha$  activity on a responsive reporter gene for which transcription is driven by an estrogen-responsive minimal promoter and enhanced by estrogen response element (ERE) sequences (ERE-TK-luc; Fig. 1B). ER $\alpha$ -negative MDA-MB-231 breast cancer cells were co-transfected with expression vectors for wt ER $\alpha$ , TAP-ER $\alpha$ , or the corresponding empty vectors (pSG5 and TAP) and ERE-TK-luc (41). E<sub>2</sub> exposure of transiently transfected cells induced luciferase activity in the presence of either ER $\alpha$  or TAP-ER $\alpha$ , although the activity of TAP-ER $\alpha$  was slightly lower than that of native ER $\alpha$  (Fig. 1B). Furthermore, we verified by [<sup>3</sup>H]E<sub>2</sub> binding and sucrose gradient ultracentrifugation that the two receptors showed similar hormone binding properties and sedimentation pattern. Results indicated that the presence of the tag does not influence these properties of the receptor (data not shown). Therefore, we generated stable cell clones in MCF-7 Tet-Off cells, an ER $\alpha$ -positive breast cancer cell line, by transfecting expression vectors for either the tag alone (TAP, control cells) or TAP-ER $\alpha$ . Of the TAP-ER $\alpha$  clones obtained, we selected for further use those showing a TAP-

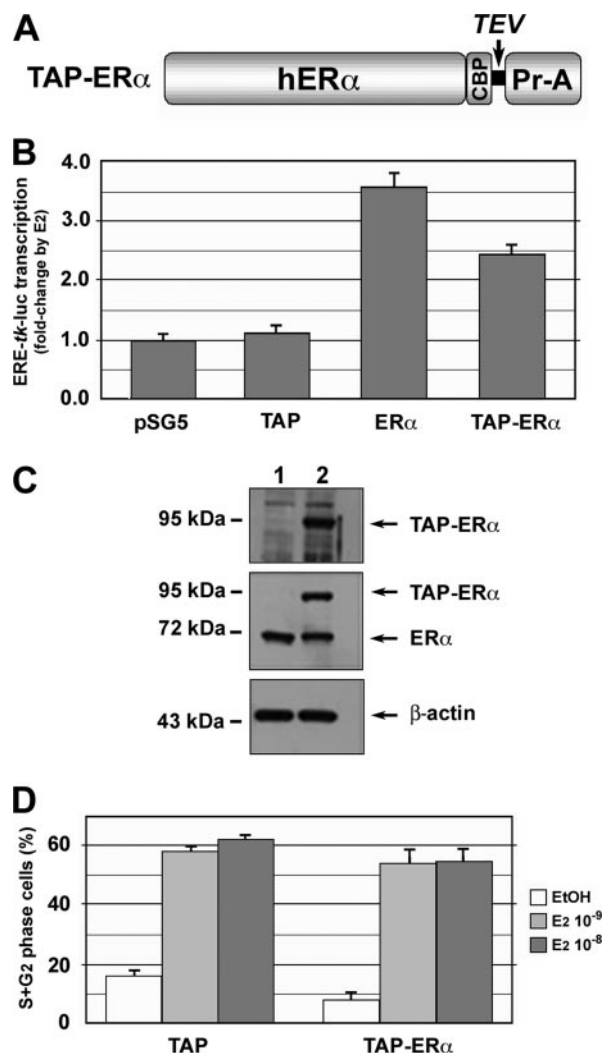


**Fig. 1. Functional analysis and stable expression in MCF-7 cells of TAP-tagged ER $\alpha$ .** A, schematic representation of the ER $\alpha$ -TAP tag fusion protein generated for this study. hER $\alpha$ , human ER $\alpha$  coding sequence (595 aa); CBP, calmodulin binding peptide (29 aa); TEV, peptide comprising a TEV protease cleavage site (18 aa); Pr-A, *Staphylococcus aureus* protein A (137 aa). B, the transcriptional activity of wt ER $\alpha$  and the TAP-ER $\alpha$  fusion protein was assayed by transient transfection in MDA-MB-231 cells. The cells, E<sub>2</sub>-deprived for 5 days, were co-transfected with the expression vectors for ER $\alpha$  and TAP-ER $\alpha$  or the respective control vectors (pSG5 and pUseAmp<sup>+</sup>C-TAP) and the reporter plasmid ERE-TK-luc; 24 h post-transfection cells were either treated with vehicle alone (control) or stimulated with E<sub>2</sub> for 24 h, and luciferase activity was assayed in whole-cell extracts. Results ( $\pm$ S.E.) are representative of two experiments performed in triplicate. C, MCF-7 cells were stably transfected with expression vectors for the TAP tag alone (lanes 1) or for TAP-ER $\alpha$  (lanes 2). The expression of the tagged receptor and its ratio to the endogenous receptor were assayed by WB of protein extracts from selected clones. Results shown refer to the cell clone used for the further experiments. D, analysis of cell cycle progression after estrogen stimulation of MCF-7-derived cell clones expressing the TAP tag alone or TAP-ER $\alpha$ . The percentage of S + G<sub>2</sub> phase cells was determined by flow cytometry in estrogen-starved cultures 27 h after treatment with vehicle alone (EtOH) or the indicated concentrations of E<sub>2</sub>. Results ( $\pm$ S.E.) are representative of three experiments performed in triplicate.

ER $\alpha$ /ER $\alpha$  ratio equal to about 1 as assessed by immunoblotting with ER $\alpha$ -specific antibodies, [ $^3$ H]E $_2$  binding, and ELISAs (Fig. 1C, *middle panel*, and data not shown). This decision was justified by the need to avoid using cells overexpressing the fusion protein to minimize possible problems due to toxic and artifactual effects caused by an excess of the exogenous fusion protein. As shown in Fig. 1D, ectopic expression of TAP-ER $\alpha$  did not affect cell cycle regulation by E $_2$  as hormone-deprived TAP and TAP-ER $\alpha$  cells exhibited similar cell cycle progression following stimulation with two different E $_2$  concentrations ( $10^{-9}$  and  $10^{-8}$  M). Furthermore, expression of the TAP-ER $\alpha$  did not influence the overall expression or nuclear translocation of endogenous ER $\alpha$  (supplemental Fig. S2) nor did it interfere with the effects of estrogen on cell proliferation and survival (data not shown). These results, combined with the observation that nuclear translocation of ER $\alpha$  and TAP-ER $\alpha$  was comparable, indicate that the TAP tag had little effect on ER $\alpha$  functions and that ectopic expression of TAP-ER $\alpha$  does not influence the normal behavior of recipient cells.

**Purification of ER $\alpha$  Nuclear Complexes and Identification of Their Protein Components**—The TAP-ER $\alpha$  clones obtained were used to purify nuclear ER $\alpha$ -binding protein complexes. To this end, cells maintained in the absence of estrogen for 5 days were exposed to E $_2$  for 2 h before preparation of nuclear extracts, which were then subjected to a first round of purification by affinity chromatography with Sepharose-bound human IgG. The beads were extensively washed, and TEV protease cleavage was used to elute the receptor and its interacting proteins according to the protocol reported in Fig. 2A. Proteins binding nonspecifically to the affinity matrix were obtained from TAP cells (Fig. 2B). Results of a representative purification carried out with TAP-ER $\alpha$  cell extracts are reported in Fig. 2C, which shows the strong reduction ( $\sim 80\%$ ) of signal relative to TAP-ER $\alpha$  following incubation of the extracts with IgG-Sepharose (compare *lanes 1* and *2*), suggesting efficient binding of the fusion protein to the affinity matrix, a result confirmed by the relatively large amount of TAP-ER $\alpha$  bound to the beads at the end of this procedure (*lane 3*). About 12–20% of TAP-ER $\alpha$  from nuclear extracts was recovered following two elution steps with TEV (*lanes 5* and *6*, CBP-ER $\alpha$ ). Interestingly, we observed that endogenous ER $\alpha$  also binds to the matrix under these conditions but only in the presence of TAP-ER $\alpha$  (Fig. 2, *B* and *C*, compare *lanes 3*) and could be eluted by TEV cleavage (Fig. 2C, *lane 5*, and data not shown). This is likely due to formation of ER $\alpha$ -TAP-ER $\alpha$  heterodimers.

The TEV eluates obtained as described above were analyzed by two-dimensional DIGE followed by LC-MS/MS analysis of specific protein spots identified (Fig. 3). Samples derived from TAP and TAP-ER $\alpha$  cells were labeled with Cy2 and Cy3 dyes, respectively, mixed, and analyzed as described under "Experimental Procedures." Upon the merge of the Cy2 and Cy3 fluorescent images, 12–15 detectable spots specific for the TAP-ER $\alpha$  sample were observed and picked, and proteins were digested with trypsin and analyzed by LC-MS/

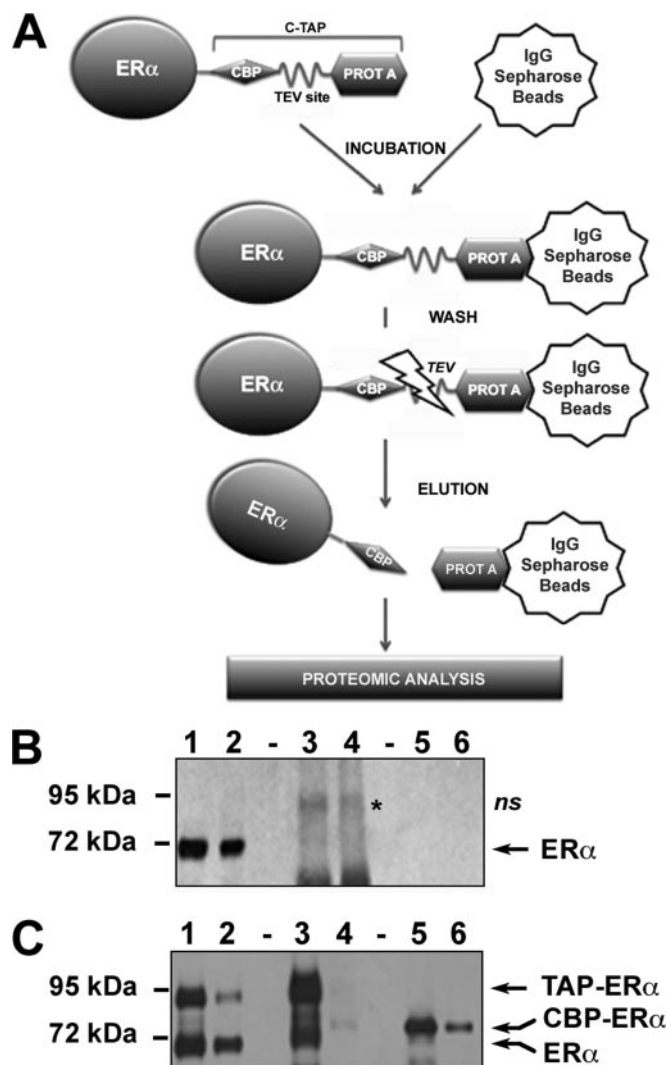


**FIG. 2. TAP-ER $\alpha$  protein complex purification.** A, schematic representation of the first steps of the tandem affinity purification procedure applied for isolation of native ER $\alpha$ -containing complexes from MCF-7 cell nuclei. B and C, nuclear extracts from TAP- (B) and TAP-ER $\alpha$  (C)-expressing cells were isolated and purified as described above, and exogenous protein recovery was monitored by WB using a specific Ab against human ER $\alpha$ . In both cases, the relative concentrations of both forms of the receptor are shown before and after addition of IgG-Sepharose (*lanes 1* and *2*), bound to IgG-Sepharose before and after TEV cleavage (*lanes 3* and *4*), and in eluates obtained by two sequential TEV treatments (*lanes 5* and *6*). To avoid saturation of the signal, different amounts of samples were loaded in each case as follows: 1:400 for nuclear extract (*lanes 1* and *2*), 1:200 for IgG bead slurry (*lanes 3* and *4*), and 1:100 for each TEV eluate (*lanes 5* and *6*). \*ns, nonspecific band detected by the Abs used; PROT A, protein A; CBP, calmodulin binding peptide.

MS. Reliable sequence data leading to unequivocal protein identification were obtained only for the four most abundant proteins circled in the *bottom panel* of Fig. 3. Three were identified as gelsolin,  $\beta$ -actin (reproducibly the most abundant protein in these samples), and nucleophosmin (spots A, B, and C, respectively, highlighted in the *bottom panel* of Fig. 3).

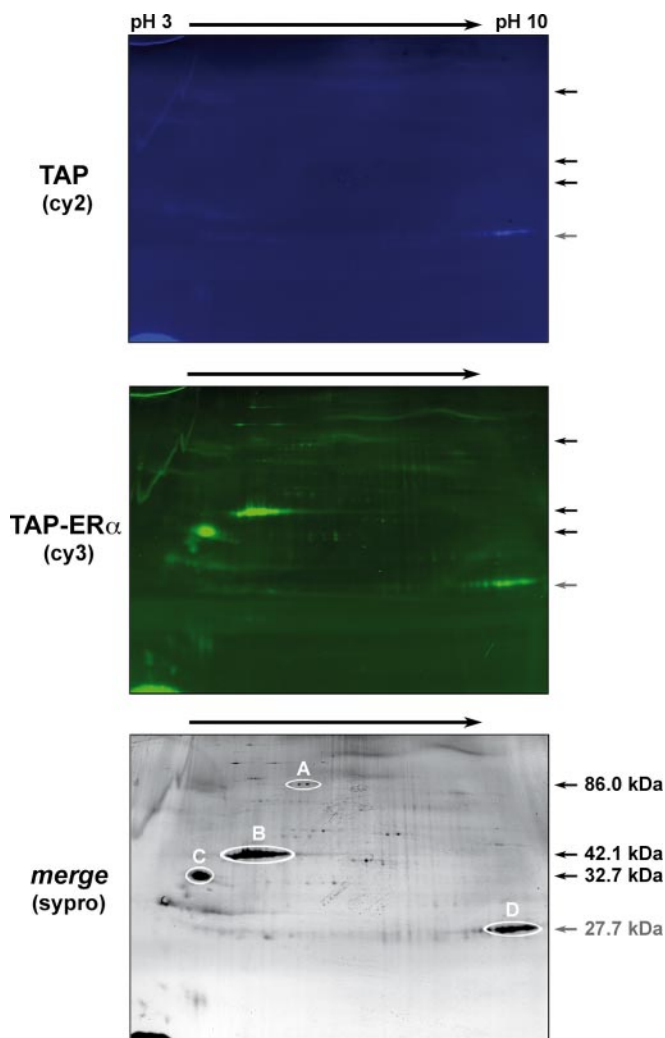


FIG. 3. DIGE two-dimensional gel of proteins after tandem affinity purification. TEV eluates were obtained by purification of nuclear proteins (50 mg) from TAP- and TAP-ER $\alpha$ -expressing cells; they were labeled with Cy2 and Cy3 dye, respectively, before separation by two-dimensional gel electrophoresis. The TAP-ER $\alpha$ -specific spots, circled in the image of the SYPRO staining (lower panel), were excised and analyzed by LC-MS/MS. The identified proteins are listed in Table I. Arrows and numbers refer to the position and molecular mass of the four proteins (A–D) identified by MS analysis.

The data that led to identification of these proteins by MS are reported in Table I, which also includes those relative to spot D, which corresponds to the TEV protease introduced in the samples for protein elution from IgG-agarose. All other spots visible in Fig. 3 did not yield reliable sequence data and were thus not considered further.

To identify additional components of these complexes, we also analyzed TEV eluates from TAP-ER $\alpha$  and, as control, TAP cells by nano-LC-MS/MS. This led to identification of a set of nuclear partners of ER $\alpha$  that was matched with that of validated  $\beta$ -actin interactors from the UniProt database (42). The resulting list of known  $\beta$ -actin-interacting proteins that copurified with ER $\alpha$ , reported in Table II, includes Arp2 and -3,

gelsolin, nucleophosmin, and myosin 1c together with the known ER $\alpha$  interactors p68 RNA helicase DDX5 (46) and heat shock 70-kDa protein 8 (HSPA8; Ref. 47). The mRNAs encoding all the proteins listed in Table II were found expressed in wt, TAP, and TAP-ER $\alpha$  MCF-7 clones by whole-genome RNA expression profiling (data not shown), confirming that the corresponding genes are indeed expressed in the cell lines used for this study. It is worth mentioning that Arp2/3 and myosin 1c have been described to have a role with  $\beta$ -actin not only in regulating RNA polymerase II activity (35, 48, 49) but also in long range chromatin interactions involving hormone-responsive genes and mediated by ER $\alpha$  (9). A recent study identified, by quantitative nanoproteomics (QNanoPX), several ERE-binding proteins from MCF-7 cell nuclei, including most of the ER $\alpha$  interactors reported in Table II (50). *In vitro* binding to ERE of a significant number of these proteins, including ER $\alpha$  itself, was found to be increased by estrogen treatment of the cells, suggesting that they might belong to multiprotein complexes also comprising the receptor. Interestingly, the list of such proteins includes  $\beta$ -actin, nucleophosmin, myosins, and several ribosomal proteins, providing an independent validation of the results obtained in our study and further evidence for the likely involvement of  $\beta$ -actin and its molecular partners in target gene regulation by ER $\alpha$ .

**Characterization of ER $\alpha$ - $\beta$ -Actin Complex Assembly**—The co-purification of nuclear  $\beta$ -actin with ER $\alpha$  is particularly interesting in view of the emerging role of  $\beta$ -actin in transcriptional regulation, spatial organization of chromatin, and functional compartmentalization of nuclei. For this reason, the nature and significance of the ER $\alpha$ - $\beta$ -actin association was investigated in detail. To examine the temporal pattern of ligand-induced ER $\alpha$  interaction with  $\beta$ -actin, TAP-ER $\alpha$ -expressing cells were hormone-starved for 5 days and then exposed to  $10^{-8}$  M E $_2$  for 15–120 min. Nuclear proteins (1 mg) were immunoprecipitated with IgG-Sepharose, and protein complexes bound to the matrix were analyzed by immunoblotting (Fig. 4A). Results showed hormone-dependent binding of  $\beta$ -actin to TAP-ER $\alpha$  detectable 15–30 min after E $_2$  exposure and increasingly thereafter in a time-dependent manner. The amount of  $\beta$ -actin found associated to the affinity matrix 60–120 min after estrogen stimulation reached a level far exceeding that of TAP-ER $\alpha$  itself. Moreover, 120 min after E $_2$  exposure high molecular weight actin species (marked by the arrows in Fig. 4A), reminiscent of SDS-resistant F-actin, were also detectable in the immunoprecipitates, suggesting that E $_2$  might promote polymerization of ER $\alpha$ -bound nuclear  $\beta$ -actin similarly to that observed previously for the free cytosolic form of this protein (43). Of note, tubulin was not detectable in our nuclear extracts, indicating the absence of cytosolic contaminations, which might impede a correct interpretation of this result (supplemental Fig. S2 and data not shown). A time- and hormone-dependent pattern of interaction with TAP-ER $\alpha$  was also observed for gelsolin, myosin 1c, nucleophosmin, and flightless I, a previously described ER $\alpha$

TABLE I

Proteins co-purified with ER $\alpha$  by IgG-Sepharose affinity chromatography and identified by two-dimensional PAGE followed by LC-MS/MS analysis

Following two-dimensional DIGE analysis of the TEV eluates shown in Fig. 3, the spots corresponding to protein species clearly detectable in ER $\alpha$ -containing samples only were cut, trypsin-digested, and subjected to LC-MS/MS analysis. The proteins identified, corresponding to spots A–D in the figure, are listed together with information relative to the MS data that led to their identification.

Protein ID (NCBI)	Protein name	Gene name	No. of peptides matched	Sequence coverage	Mowse score
				%	
A	gi 119607896	Gelsolin	6	10	230
B	gi 4501885	$\beta$ -Actin	6	19	234
C	gi 10835063	Nucleophosmin	10	32	477
D	gi 25013638	Nla-Pro protein (tobacco etch virus)	2	10	142

TABLE II

Known  $\beta$ -actin-interacting proteins co-purified with ER $\alpha$  by IgG-Sepharose affinity chromatography and identified by nano-LC-MS/MS analysis

The list of  $\beta$ -actin-interacting proteins from the UniHI database was crossed with the list of proteins co-purified with TAP-ER $\alpha$ , but not with the TAP tag alone, and identified by nano-LC-MS/MS analysis of purified samples. Proteins are listed with information relative to the MS data that led to their identification. Two identified proteins not listed as validated direct interactors of actin in the UniHI database and ER $\alpha$  itself are reported in bold. n/a, not applicable.

Protein ID (Swiss-Prot)	Protein name	Gene name	No. of peptides matched	Sequence coverage	Mowse score	Confirmed by WB
				%		
<b>P03372</b>	<b>Estrogen receptor</b>	<b>ESR1</b>	<b>2</b>	<b>6</b>	<b>97</b>	<b>n/a</b>
P60709	Actin, cytoplasmic 1	ACTB	20	53	2509	+
P68032	Actin, $\alpha$ cardiac muscle 1	ACTC1	14	24	1901	
P11142	Heat shock cognate 71-kDa protein	HSPA8	9	18	294	
P06748	Nucleophosmin	NPM1	9	31	234	+
Q07020	60 S ribosomal protein L18	RPL18	5	24	206	
P17844	Probable ATP-dependent RNA helicase DDX5	DDX5	14	22	182	+
P05388	60 S acidic ribosomal protein P0	RPLP0	9	39	180	
P62424	60 S ribosomal protein L7a	RPL7A	7	19	113	
P60660	Myosin light polypeptide 6	MYL6	4	30	104	
P18124	60 S ribosomal protein L7	RPL7	6	25	88	
P62701	40 S ribosomal protein S4, X isoform	RPS4X	8	26	79	
P06396	Gelsolin	GSN	5	6	77	+
O00159	Myosin 1c	MYO1C	9	9	72	+
O00571	ATP-dependent RNA helicase DDX3X	DDX3X	4	5	71	
P46781	40 S ribosomal protein S9	RPS9	7	29	62	
P62241	40 S ribosomal protein S8	RPS8	4	21	61	
<b>P61158</b>	<b>Actin-related protein 3</b>	<b>ACTR3</b>	<b>2</b>	<b>7</b>	<b>58</b>	<b>+</b>
<b>P61160<sup>a</sup></b>	<b>Actin-related protein 2</b>	<b>ACTR2</b>	<b>1</b>	<b>1</b>	<b>32</b>	<b>+</b>

<sup>a</sup> Raw MS/MS fragmentation data and Mascot search results included as supplemental data.

cofactor (51, 52). The TAP-ER $\alpha$ - $\beta$  actin complex could be detected only in the nucleus of hormone-stimulated cells as IgG affinity chromatography of TAP-tagged ER $\alpha$  present in the cytoplasmic fraction from the same cells failed to show TAP-ER $\alpha$ -associated  $\beta$ -actin (Fig. 4B).

Specificity of the interaction between ER $\alpha$  and  $\beta$ -actin was also verified by other means. First of all, we investigated E<sub>2</sub>-dependent co-immunoprecipitation of the two proteins in cells expressing FLAG- $\beta$ -actin (Fig. 5A). In this case, wt MCF-7 cells were E<sub>2</sub>-starved, transfected with an expression vector encoding FLAG- $\beta$ -actin, and exposed to vehicle alone (ethanol (EtOH); Fig. 5A, upper panel) or to 10<sup>-8</sup> M E<sub>2</sub> (Fig. 5A, bottom panel) for 1 h before extraction and immunoprecipitation of nuclear proteins with an anti-FLAG affinity matrix.

Results showed that endogenous ER $\alpha$  readily binds to FLAG- $\beta$ -actin only in the presence of hormone (Fig. 5A, compare lanes 3 and 4 with lanes 7 and 8). We then searched for evidence of naturally occurring interactions between endogenous proteins in exponentially growing MCF-7 cells. Nuclear extracts prepared from cells maintained in normal growth medium (containing estrogen) were immunoprecipitated with an Ab against wt ER $\alpha$  and analyzed by WB with Abs specific for  $\beta$ -actin, flightless I, gelsolin, myosin 1c, and nucleophosmin. The results, shown in Fig. 5B, indicated steady-state association of all proteins analyzed with ER $\alpha$  under these conditions, confirming what was observed by purification of TAP-ER $\alpha$  complexes and during early stimulation of hormone-starved cells with E<sub>2</sub>. We confirmed  $\beta$ -actin interaction with



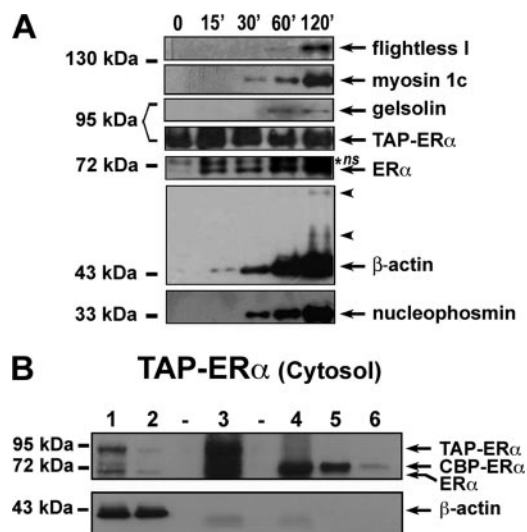


**FIG. 4. 17 $\beta$ -Estradiol promotes time-dependent recruitment of  $\beta$ -actin and actin-interacting proteins to TAP-ER $\alpha$  in MCF-7 cell nuclei.** A, TAP-ER $\alpha$ -expressing cells were E $_2$ -deprived (0) and subsequently stimulated for the indicated times (', minutes), and 1 mg of nuclear proteins was incubated in each case with IgG-Sepharose and, upon binding and extensive washing, directly analyzed by WB, probing the membrane with specific Abs for the indicated proteins. The results shown in the figure were obtained on the same membrane and are representative of replicate experiments. B, cytoplasmic extracts (50 mg) prepared from TAP-ER $\alpha$ -expressing cells stimulated with E $_2$  for 2 h were prepared as described under "Experimental Procedures" and processed as reported in Fig. 2A. To avoid saturation of the signal, different amounts of samples were loaded in each case as follows: 1:400 for cytosolic extract (lanes 1 and 2), 1:40 for IgG bead slurry (lanes 3 and 4), and 1:25 for each TEV eluate (lanes 5 and 6). \*ns, nonspecific band detected by the Abs used.

ER $\alpha$  also in wt MCF-7 cells transiently transfected with expression vectors encoding either FLAG- $\beta$ -actin (Fig. 5C, left panel) or FLAG-ER $\alpha$  (Fig. 5C, right panel). In these experiments, we also confirmed by WB interaction of Arp2 and -3, which are known to play a key role in actin nucleation and function in the nucleus (33, 34), with ER $\alpha$ .

To evaluate the possible functional significance of the ER $\alpha$ - $\beta$ -actin interaction observed *in vitro*, we investigated whether the two proteins can co-localize at a specific active chromatin site *in vivo*. To this end, we measured by ChIP E $_2$ -dependent loading of ER $\alpha$  and  $\beta$ -actin onto a receptor binding site located upstream of the E $_2$ -responsive pS2/*TFE1* gene promoter. For this, chromatin was prepared from E $_2$ -starved MCF-7 cells treated with vehicle (EtOH) or E $_2$  for 45 min and immunoprecipitated with anti-ER $\alpha$ , anti- $\beta$ -actin, or beads alone (no Ab; to define the background). As shown in Fig. 6A, E $_2$  stimulation induced loading of both  $\beta$ -actin and ER $\alpha$  onto the ERE-containing pS2 promoter, suggesting a functional association of the two proteins at this site.

The role of the ligand in ER $\alpha$ - $\beta$ -actin complex formation was tested with 4-hydroxytamoxifen (Tam), a partial ER $\alpha$  antagonist that induces specific conformational changes of the receptor molecule that do not affect its ability to translocate in

the nucleus or to bind DNA but influences its specific interaction with co-regulators (22, 53). E $_2$ -starved TAP-ER $\alpha$  cells were exposed to either E $_2$  or Tam ( $10^{-8}$  M), and receptor binding to  $\beta$ -actin was measured in nuclear extracts by IgG-Sepharose chromatography and WB. Results showed comparable ER accumulation in the nucleus (Fig. 6B, lanes 1 and 4) and formation of ER $\alpha$ -TAP-ER $\alpha$  heterodimers as well as receptor binding to  $\beta$ -actin in response to the two ligands (Fig. 6B, compare lanes 2 and 3 and lanes 5 and 6). As the efficiency and kinetics of  $\beta$ -actin recruitment to the receptor were similar (data not shown), we concluded that the differential conformations of ER $\alpha$  elicited by E $_2$  and Tam (54) are not relevant for receptor interaction with  $\beta$ -actin. These data also suggest that nuclear translocation and binding to chromatin likely play a role in the association between ER $\alpha$  and  $\beta$ -actin.

It has been shown that  $\beta$ -actin interaction with the transcriptional machinery is linked to its polymerization status that, in turn, depends upon the cell activation state (55). For this reason, we considered the possibility that nuclear  $\beta$ -actin polymerization may play an active role also in ER $\alpha$ -dependent transcriptional regulation. We thus assessed the effects on ER-mediated promoter *trans*-activation of cytochalasin D (Cyt D), a drug that induces depolymerization of the  $\beta$ -actin cytoskeleton (56) and is able to interfere with  $\beta$ -actin effects in *in vitro* transcription assays (55, 57). For this, MELN cells were used as they carry an ERE-luciferase reporter gene stably integrated in the genome (38). Cells were deprived from estrogen and then exposed to vehicle alone (EtOH), E $_2$  ( $10^{-9}$  M), or Tam ( $10^{-9}$  M) in the presence and absence of Cyt D (5  $\mu$ M). As shown in Fig. 6C, the drug had no major effects on E $_2$ -mediated activation of the reporter, suggesting that efficient actin polymerization may not be a critical step in transcription enhancement by ER $\alpha$  at least in this experimental model. On the other hand, Cyt D alone induced activation of the reporter gene (Fig. 6C, see Cyt D + EtOH). This apparently surprising effect of the drug may be explained by its ability to induce mobilization of monomeric  $\beta$ -actin in the cytoplasm from where it can easily migrate to the nucleus and engage with the basal transcription machinery (34, 36, 58), a possibility further supported by the fact that the effect of Cyt D on reporter gene activity was additive to that of E $_2$  and independent from the presence of Tam, which in this context acts mainly as an estrogen antagonist. Comparable results were obtained in HeLa cells carrying human ER $\alpha$  upon transient transfection of the ERE-TK-luciferase reporter gene (data not shown).

**Molecular Characterization of ER $\alpha$ -associated Components of Nuclear  $\beta$ -Actin Network**—In the nucleus,  $\beta$ -actin exerts its multifaceted activities by dynamically shifting from a globular (G) to a filamentous (F) form in response to intra- and extracellular stimuli accompanied by its association with various proteins and multiprotein complexes. The data reported in Fig. 4 indicate that the number of actin molecules associated with the receptor increases progressively with time after E $_2$  stimulation, reaching a large molar excess with respect to

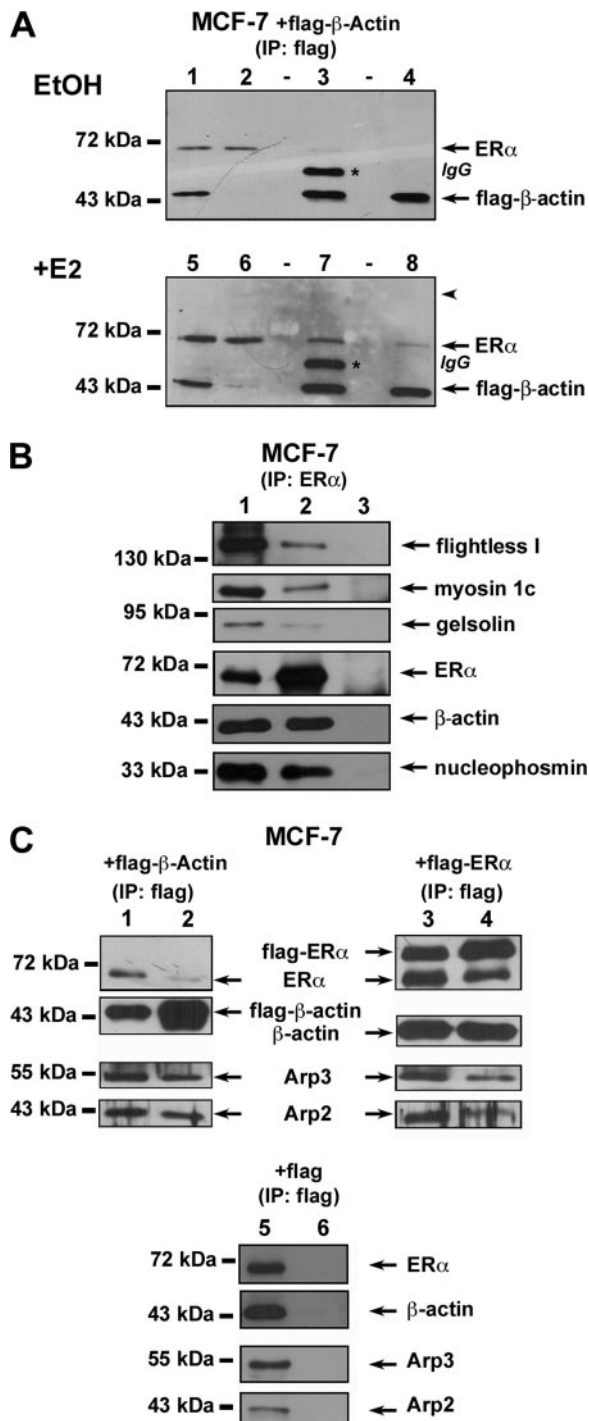


**FIG. 5. Hormone-dependent association of ER $\alpha$ ,  $\beta$ -actin, and actin-interacting proteins in MCF-7 cell nuclei.** *A*, hormone-starved MCF-7 cells were transfected with an expression vector encoding FLAG- $\beta$ -actin and treated either with EtOH (negative control) or  $10^{-8}$  M E $_2$  for 1 h. Nuclear extracts (0.5 mg of proteins) were immunoprecipitated (IP) with anti-FLAG Abs and analyzed by WB with either anti-FLAG or anti-ER $\alpha$  Abs. Samples analyzed are as follows: nuclear extracts before (lanes 1 and 5) and after (lanes 2 and 6) incubation with the affinity resin and bound (lanes 3 and 7) and eluted (lanes 4 and 8) proteins. *B*, MCF-7 nuclear extracts (0.5 mg of protein;

ER $\alpha$  and clearly comprising high molecular weight species. We thus evaluated directly *in vivo* association of ER $\alpha$  with G- and F- $\beta$ -actin-fractionating nuclear extracts from MCF-7 cells by ultracentrifugation followed by WB analysis of the G- and F-actin-containing fractions. As shown in Fig. 7A, ER $\alpha$  was found almost completely associated with nuclear F-actin in cells under normal growth conditions. Therefore, we decided to analyze by glycerol gradient centrifugation the sedimentation pattern of ER $\alpha$  and  $\beta$ -actin in nuclear extracts prepared from hormone-starved and TAP-ER $\alpha$  cells exposed to E $_2$  ( $10^{-8}$  M) for 2 h. The sedimentation profiles of ER $\alpha$  and TAP-ER $\alpha$  reported in Fig. 7B are coincident and show the presence of very large species (>18 S), sedimenting at the bottom of the gradient, and lighter ones, showing a broad peak at fractions 3–11. The sedimentation profiles of  $\beta$ -actin was similar to that of ER $\alpha$  with both proteins sedimenting predominantly in the first third of the gradient and at the bottom where large F-actin polymers and multiprotein complexes are likely to be found. Interestingly, gelsolin, myosin 1c, and nucleophosmin showed a similar distribution in the gradient (Fig. 7B). The sedimentation pattern of all these proteins in purified samples showed a net prevalence for the largest molecular species characterized by a very high sedimentation coefficient (Fig. 7C). When combined, these results indicate that in nuclear extracts from estrogen-stimulated MCF-7 cells ER $\alpha$  and  $\beta$ -actin can be found together in large and possibly heterogeneous complexes, comprising also other components of the nuclear  $\beta$ -actin network, and that the purification protocol for this study allows purification and analysis of such complexes.

Focusing on gelsolin, flightless I, and myosin 1c, we then performed an analysis aimed at investigating their role in assembly, stability, and/or stoichiometry of the  $\beta$ -actin-ER $\alpha$  complex. These proteins were chosen as they are all known to be involved in both regulation of gene transcription and assembly/function of the nuclear F-actin network. For this experiment, we generated mutant MCF-7 cell clones where gelsolin (GSN<sup>K $\alpha$</sup> ), flightless I (FLII<sup>K $\alpha$</sup> ), or myosin 1c (MYO<sup>K $\alpha$</sup> ) levels in the cell were knocked down by lentivirus-mediated stable transduction of gene-specific shRNAs. Lentiviral vectors targeting different portions of each transcript were used to infect MCF-7 cells to generate stable clones, which were

lane 1) were immunoprecipitated with anti-ER $\alpha$  Abs (lane 2) or unrelated antibodies (anti-green fluorescent protein; lane 3) and analyzed by WB, probing the membrane with specific Abs for the indicated proteins. The results obtained on the same membrane are shown in the figure and are representative of results obtained in multiple experiments. *C*, hormone-starved MCF-7 cells were transfected with the expression vectors for either FLAG- $\beta$ -actin, FLAG-ER $\alpha$ , or FLAG alone (p3XFLAG-CMV) and stimulated with  $10^{-8}$  M E $_2$  for 1 h. Nuclear extracts (lanes 1, 3, and 5) were immunoprecipitated with anti-FLAG Abs, and the immunoprecipitates were analyzed by WB for the presence of the indicated proteins (lanes 2, 4, and 6). The data shown are representative of two experiments and were obtained by hybridization of the same membrane with the indicated Abs.

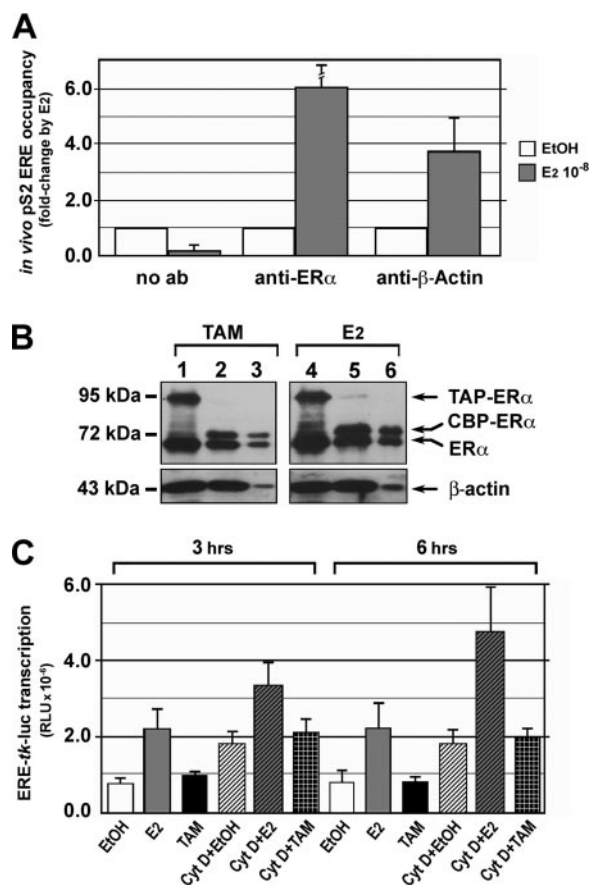


**FIG. 6.** *In vivo* co-localization of ER $\alpha$  and  $\beta$ -actin on the E $_2$ -responsive pS2/TFF1 gene promoter following estrogen stimulation, induction of ER $\alpha$ - $\beta$ -actin complex formation by tamoxifen and effects of cytochalasin D on ER-mediated gene activation. **A**, ChIP experiments were performed on chromatin prepared from MCF-7 cells deprived of hormone and stimulated with EtOH or  $10^{-8}$  M E $_2$  for 45 min before *in vivo* chromatin cross-linking, extraction, immunoprecipitation, and analysis as described under "Experimental Procedures." no ab, negative control. The results refer to replicate experiments carried out in triplicate ( $\pm$ S.E.). **B**, nuclear extracts were prepared from TAP-ER $\alpha$ -expressing cells that were hormone-starved and then treated with  $10^{-8}$  M E $_2$  or tamoxifen (TAM) for 45 min. 7 mg of proteins were subjected to IgG-Sepharose binding and TEV elution before WB with specific Abs against the indicated proteins. IgG-bound samples (lanes 1 and 4), IgG-bound samples after TEV cleavage (lanes 2 and 5), TEV-eluted samples (lanes 3 and 6) are shown. **C**, MELN, MCF-7 cells carrying the luciferase gene under the control of a minimal E $_2$ -responsive promoter stably integrated in the genome, were hormone-starved for 5 days before treatment for the indicated times with EtOH, E $_2$ , or tamoxifen. Where indicated, Cyt D ( $5 \mu$ M) was added to the cultures either 3 h before (3-h time point) or together with EtOH or ER ligands (6-h time point), and cells were harvested at the indicated times for analysis of luciferase activity. Luciferase activity values reported were normalized to the protein content of each extract. Results ( $\pm$ S.E.) are representative of two experiments performed in triplicate. CBP, calmodulin binding peptide; RLU, relative light units.

then individually tested by quantitative RT-PCR and Western blotting for expression of the targeted mRNAs and proteins. One clone for flightless I (Fig. 8) and two clones each for

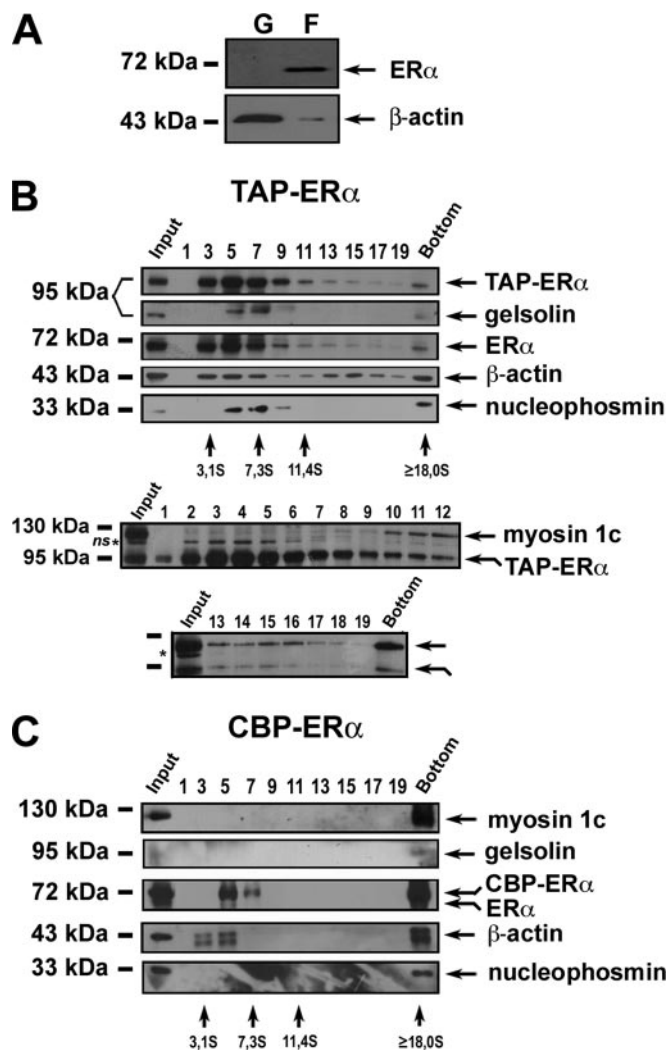


**FIG. 7.** Association of hormone-activated ER $\alpha$  to F-actin and evidence for high molecular weight ER-containing complexes in crude and affinity-purified nuclear extracts from hormone-stimulated MCF-7 cells. **A**, association of ER $\alpha$  to F-actin was assayed in MCF-7 cells under normal growing conditions. Nuclei from actively growing cells were prepared as reported under "Experimental Procedures" and processed to separate G- and F-actin. The separated fractions were analyzed by WB. **B** and **C**, nuclear extracts (2 mg of proteins; **B**) or IgG-Sepharose-purified samples (40  $\mu$ g of TEV eluate proteins; **C**) from hormone-starved TAP-ER $\alpha$  cells stimulated with E $_2$  ( $10^{-8}$  M) for 2 h were fractionated on 5–45% glycerol gradients as described under "Experimental Procedures." 0.5-ml fractions were collected from the top of each gradient, and 30- $\mu$ l aliquots of the indicated fractions were analyzed by WB. The data shown in both panels are representative of two experiments and were obtained by hybridization of the same membrane with the indicated Abs with the exception of data relative to myosin 1c in **B**. ns\*, nonspecific band detected by anti-myosin 1c Abs; CBP, calmodulin binding peptide.

gelsolin and myosin 1c (Fig. 8 and supplemental Fig. S3) showed significant targeted protein depletion and were propagated and used for further testing. Nuclear extracts were prepared from exponentially growing wt or mutated (knock-down) cells, immunoprecipitated with anti-ER $\alpha$  antibodies,

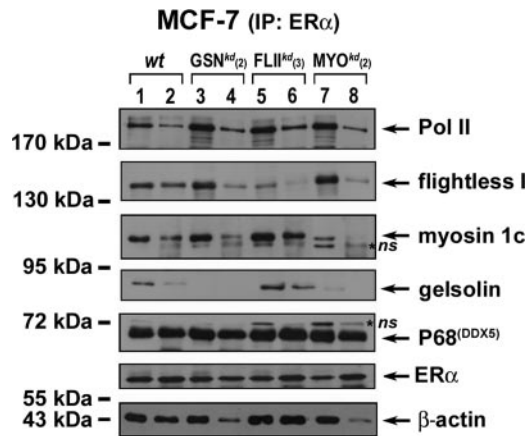


FIG. 8. Lentivirus-mediated gene knockdown analysis of role of gelsolin, flightless I, and myosin 1c in ER $\alpha$ - $\beta$ -actin complex formation. MCF-7 cells were infected with lentiviruses expressing shRNA for gelsolin (GSN<sup>kd(2)</sup>), flightless I (FLII<sup>kd(3)</sup>), and myosin 1c (MYO<sup>kd(2)</sup>). Nuclear extracts (1 mg) from control (Ctrl) or knockdown cells maintained under normal growing conditions were immunoprecipitated (IP) with an anti-ER $\alpha$  Ab. Nuclear extracts (lanes 1, 3, 5, and 7) and immunoprecipitated samples (lanes 2, 4, 6, and 8) were analyzed by WB, probing the membrane with specific Abs for the indicated proteins. Results obtained on the same membrane are shown in the figure and are representative of two independent infections and, in each case, of replicate analyses. \*ns, nonspecific band detected by the Abs used; Pol, RNA polymerase.

and analyzed by WB. The results reported in Fig. 8 show that although decreased cellular levels of flightless I did not interfere with the ER $\alpha$ / $\beta$ -actin ratio in the immunoprecipitates (compare lanes 2 and 6) knockdown of gelsolin caused a significant reduction of the amount of  $\beta$ -actin that co-precipitated with the receptor (compare lanes 2 and 4). This effect of gelsolin was specific because association of all other proteins tested was unaffected, and it was detectable also in GSN<sup>kd(1)</sup> cells despite the fact that these cells showed a less pronounced gelsolin depletion (supplemental Fig. S3), suggesting that this result was independent from the sequence of the targeting shRNA used (supplemental Fig. S3, lanes 2 and 4). The most likely explanation for this result is that a reduction of the gelsolin levels in the nucleus either prevents efficient  $\beta$ -actin binding to ER $\alpha$  or interferes with receptor-associated  $\beta$ -actin polymerization. Interestingly, myosin 1c knockdown resulted in a significant reduction of the gelsolin concentration in the cell accompanied by a comparable reduction in the amount of  $\beta$ -actin associated with the receptor (compare lanes 2 and 8). This result, which was obtained in two independent MYO<sup>kd</sup> MCF-7 cell clones and was thus independent from the sequence of shRNAs targeting myosin 1c mRNA (supplemental Fig. S3), suggests a role of this motor protein in gelsolin synthesis or turnover within the cell and confirms, indirectly, the results obtained in GSN<sup>kd</sup> cells. By comparing two MYO<sup>kd</sup> clones showing different myosin 1c levels, it was once again possible to relate the relative amount of myosin 1c with that of  $\beta$ -actin associated with ER $\alpha$  (supplemental Fig. S3).

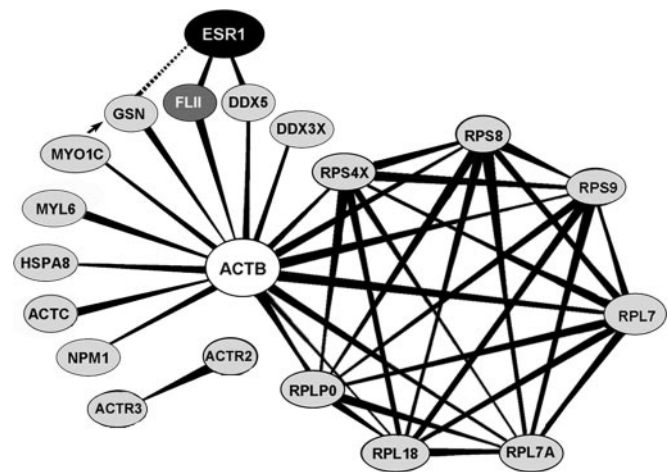


FIG. 9. Identification of ER $\alpha$ - $\beta$ -actin protein network in hormone-stimulated MCF-7 cell nuclei. To draw the map of ER $\alpha$  and  $\beta$ -actin interactions, the list of proteins identified by mass spectrometry analysis of IgG-Sepharose-purified TAP-ER $\alpha$  samples was matched to the list of known  $\beta$ -actin-interacting proteins present in the UniHI database. Solid lines connecting proteins mark direct protein-protein interactions. FLII is reported in gray because it was identified in this study by WB but not by MS analysis; the dotted line and the arrow recapitulate the experimental results described here.

The results of this study, combined with information relative to direct protein-protein interactions retrieved from the UniHI database, have been summarized in Fig. 9 in the form of a protein network. The broken line connecting ER and gelsolin indicates that knockdown of this protein impaired the naturally occurring interaction between ER $\alpha$  and  $\beta$ -actin even when it was the indirect result of myosin 1c knockdown (highlighted by the arrow). Flightless I has been included in the network although it has not yet been identified by MS analysis because it is a known ER cofactor in breast cancer cells (51, 52), and its presence in our purified samples was confirmed by immunoblotting. This data visualization method reveals also that seven of the novel ER-interacting proteins identified, all involved in assembly of the ribosome (59, 60) and RNA translocation processes (61, 62), are tightly interconnected with each other and appear to group as a distinct component of this ER $\alpha$ -associated nuclear protein network.

#### DISCUSSION

Significant efforts have been spent to date to identify genes and proteins that play a role in estrogen control of hormone-responsive breast cancer cell functions via ERs. Gene expression profiling and genetic and molecular approaches have identified several proteins involved in the ER-mediated signaling and regulation of target gene transcription (63–65). The nucleus is the main site of action of these receptors, and the involvement of nuclear proteins in ER-mediated signaling in this cellular compartment has been extensively studied in BC and other hormone-responsive cell models, leading to the identification of molecular partners of ERs, including components of the basal transcription machinery and the protea-

some-mediated degradation pathway and chromatin remodeling complexes (66–69). These results led, among others, to a model for promoter *trans*-activation by ER $\alpha$  based on multiple cycles of multiprotein complex recruitment onto gene control regions by sequential assembly and clearance consequent to recruitment of proteasome components and HSPA8 (70). The full list of molecular players in such a process, however, is not yet known. Moreover, several other effects of ligand-activated ERs in the nucleus have been described that are likely to involve several ER-interacting molecules still to be discovered, including for example control of RNA splicing, microRNA and ribosome biogenesis, and long range effects in chromatin, including remodeling and induction of physical and functional interactions between distant loci in the same or different chromosomes (9).

In this study, we decided to investigate the protein networks involving ER $\alpha$  in BC cells by beginning a comprehensive mapping of the nuclear ER $\alpha$  interactome by TAP. While pursuing this aim, we identified a set of proteins co-purifying with ligand-activated ER $\alpha$  and comprising, in particular,  $\beta$ -actin and several proteins involved in the control of actin polymerization and functions in the nucleus (Arp2 and -3, flightless I, gelsolin, myosin 1c, etc.) as well as several ribosomal proteins and regulators of ribosome biogenesis. The first group of these ER interactors plays a role in actin microfilament organization/dynamics, and some of them, mainly gelsolin, myosin 1c, and  $\beta$ -actin itself, are also involved in regulation of gene transcription (33, 53), including that mediated by estrogen in BC cells. Focusing on this set of ER-associated proteins, we found that their interaction with the receptor is dynamic and does not occur in the absence of hormone, requiring instead the presence of ligands, such as E<sub>2</sub> and Tam, that induce ER activation and nuclear translocation. Glycerol gradient centrifugation of crude and partially purified samples showed the presence of ER in complexes of various sizes, including very large complexes migrating to the bottom of the gradients and also containing  $\beta$ -actin and several of its nuclear partners. This suggests association of ER $\alpha$  with nuclear F-actin, a result confirmed experimentally in this study where F-actin polymerization also appeared to be induced by hormonal treatment of the cell, indicating a role of activated ER in this process.

ER $\alpha$  and nuclear  $\beta$ -actin both regulate multiple steps of transcription: preinitiation complex formation and its loading onto the promoter (50), elongation and premessenger RNP organization (54, 61), and ATP-dependent chromatin remodeling (33, 34). It is thus possible that ER and  $\beta$ -actin cooperate in achieving these effects in hormone-stimulated cells in particular when ER binding to the genome occurs at a distance from the target gene promoter. It has been proposed that  $\beta$ -actin plays a major role as an allosteric regulator of dynamic macromolecular complex remodeling during transcription, allowing coordination of its sequential steps. Indeed,  $\beta$ -actin-myosin 1c complexes have been shown to be involved in the transition from initiation to elongation complexes presumably

by triggering a structural change of the transcriptional apparatus (71). Interestingly, ER $\alpha$  also plays a role in such transition (72), again suggesting that both these proteins, once associated, may cooperate with each other to regulate transcription. In its G form, for example,  $\beta$ -actin could be involved in the first unproductive cycle in ER-induced transcription (70, 72), whereas recruitment of proteins involved in  $\beta$ -actin polymerization (Arp2 and -3) and F-actin filament stabilization and dynamics (myosin 1c) promoted by ER $\alpha$  could play a role in the subsequent productive cycles (73, 74). Furthermore, the interaction between chromatin remodeling complexes and nuclear F-actin has been proposed as part of the mechanism targeting these complexes to the nuclear matrix, and F-actin depolymerization appears to be required for chromatin modifier release from messenger RNP complexes concomitantly with transcription termination (74, 75). Based on all these results, interaction of ER $\alpha$  with  $\beta$ -actin could be part of the mechanisms for dynamic remodeling of multiprotein complexes during estrogen-regulated transcription (70) as well as for long range effects of ER on chromatin and repositioning of ER-responsive genes within the nucleus (9). On the other hand, inhibition of actin polymerization by Cyt D did not prevent E<sub>2</sub>-mediated activation of an artificial responsive gene carrying an ERE proximal to a minimal test promoter. This would suggest that efficient actin polymerization may not be a critical step in promotion of transcription initiation and enhancement by ER when this is acting in the proximity of a promoter. This is also suggested by the observation that reduced cellular levels of gelsolin and myosin 1c did not cause significant reduction of ER $\alpha$ -mediated *trans*-activation of a luciferase reporter gene containing a promoter-proximal ERE (data not shown).

The list of the other  $\beta$ -actin-interacting proteins co-purified with the receptor and identified in this study (Table II and Fig. 9) include several ribosomal proteins and nucleophosmin, a regulator of ribosomal biogenesis that acts by inducing rDNA transcription and preribosomal particle maturation (76). Several of these proteins have been found to be associated to transcribed loci and to play a role in regulation of gene transcription, cell proliferation, and apoptosis (62, 77), and RPL7 was shown to interact also with the vitamin D receptor, another member of the nuclear receptor family of *trans*-acting factors, to regulate gene transcription (78). Estrogen is known to control rDNA transcription (79), and E<sub>2</sub> binding sites and ER $\alpha$  itself have been shown in different cell types to localize in nucleoli or to be involved in RNP transport (80–83). The interaction between ER $\alpha$ ,  $\beta$ -actin, nucleophosmin, and the ribosomal proteins described here could thus reflect a direct molecular link between the mitogenic action of estrogen and ribosome biogenesis in BC cells. This possibility is suggested also by the known role of  $\beta$ -actin in ribosome biogenesis and maturation (71). On the other hand, several other functions have been recently associated to ribosomal proteins (84), some of which might also be relevant for estrogen control of

BC cell functions and will now be investigated in detail. In conclusion, the results of this study reveal the existence of a physical interaction in the nucleus between ligand-activated ER $\alpha$ ,  $\beta$ -actin, and several actin-binding proteins that is likely to play important functions in the genomic actions of estrogen in BC cells.

**Acknowledgments**—We are grateful to Drs. Giulio Superti-Furga and Guido Posern for kindly providing TAP and FLAG- $\beta$ -actin expression vectors, Dr. Patrick Balaguer for MELN cells, and Drs. Rosario Casale and Claudia Mastini for technical assistance. We are also grateful to the Centro Regionale di Competenza in Genomics for Applied Research for the two-dimensional DIGE facility.

\* This work was supported in part by European Union CRE-SCENDO Integrated Project Contract LSHM-CT2005-018652, Associazione Italiana per la Ricerca sul Cancro Grant IG-8586, Regione Campania and Ministero dell'Istruzione, dell'Università e della Ricerca Grant PRIN 2008CJ4SYW\_004, and the Ph.D. programs "Design and Use of Biomolecules of Biotechnological Interest" (to A. B.) and "Pathology of Cell Signal Transduction" (to G. N.) of the Second University of Naples and "Toxicology, Oncology and Molecular Pathology" of the University of Cagliari (to M. R.).

§ This article contains supplemental Figs. S1–S3.

† Recipient of a postdoctoral fellowship from the AIRC Naples Oncogenomics Center.

<sup>k</sup> To whom correspondence should be addressed: Dipartimento di Patologia generale, Seconda Università degli Studi di Napoli, vico L. De Crecchio 7, 80138 Napoli, Italy. Tel./Fax: 39-081-441655; E-mail: alessandro.weisz@unina2.it.

#### REFERENCES

- Russo, J., and Russo, I. H. (2008) Breast development, hormones and cancer. *Adv. Exp. Med. Biol.* **630**, 52–56
- Heldring, N., Pike, A., Andersson, S., Matthews, J., Cheng, G., Hartman, J., Tujague, M., Ström, A., Treuter, E., Warner, M., and Gustafsson, J. A. (2007) Estrogen receptors: how do they signal and what are their targets. *Physiol. Rev.* **87**, 905–931
- Silva, C. M., and Shupnik, M. A. (2007) Integration of steroid and growth factor pathways in breast cancer: focus on signal transducers and activators of transcription and their potential role in resistance. *Mol. Endocrinol.* **21**, 1499–1512
- Levin, E. R., and Pietras, R. J. (2008) Estrogen receptors outside the nucleus in breast cancer. *Breast Cancer Res. Treat.* **108**, 351–361
- Ciocca, D. R., and Fanelli, M. A. (1997) Estrogen receptors and cell proliferation in breast cancer. *Trends Endocrinol. Metab.* **8**, 313–321
- Manavathi, B., and Kumar, R. (2006) Steering estrogen signals from the plasma membrane to the nucleus: two sides of the coin. *J. Cell. Physiol.* **207**, 594–604
- Watson, C. S., Alyea, R. A., Jeng, Y. J., and Kochukov, M. Y. (2007) Nongenomic actions of low concentration estrogens and xenoestrogens on multiple tissues. *Mol. Cell. Endocrinol.* **274**, 1–7
- Prossnitz, E. R., and Maggiolini, M. (2009) Mechanisms of estrogen signaling and gene expression via GPR30. *Mol. Cell. Endocrinol.* **308**, 32–38
- Hu, Q., Kwon, Y. S., Nunez, E., Cardamone, M. D., Hutt, K. R., Ohgi, K. A., Garcia-Bassets, I., Rose, D. W., Glass, C. K., Rosenfeld, M. G., and Fu, X. D. (2008) Enhancing nuclear receptor-induced transcription requires nuclear motor and LSD1-dependent gene networking in interchromatin granules. *Proc. Natl. Acad. Sci. U.S.A.* **105**, 19199–19204
- Rosenfeld, M. G., Lunyak, V. V., and Glass, C. K. (2006) Sensors and signals: a coactivator/corepressor/epigenetic code for integrating signal-dependent programs of transcriptional response. *Genes Dev.* **20**, 1405–1428
- Kuiper, G. G., Carlsson, B., Grandien, K., Enmark, E., Häggblad, J., Nilsson, S., and Gustafsson, J. A. (1997) Comparison of the ligand binding specificity and transcript tissue distribution of estrogen receptors alpha and beta. *Endocrinology* **138**, 863–870
- Kuiper, G. G., Shughrue, P. J., Merchenthaler, I., and Gustafsson, J. A. (1998) The estrogen receptor beta subtype: a novel mediator of estrogen action in neuroendocrine systems. *Front. Neuroendocrinol.* **19**, 253–286
- Cheskis, B. J., Greger, J. G., Nagpal, S., and Freedman, L. P. (2007) Signaling by estrogens. *J. Cell. Physiol.* **213**, 610–617
- Syed, F. A., Fraser, D. G., Spelsberg, T. C., Rosen, C. J., Krust, A., Chambon, P., Jameson, J. L., and Khosla, S. (2007) Effects of loss of classical estrogen response element signaling on bone in male mice. *Endocrinology* **148**, 1902–1910
- Spiegelman, B. M., and Heinrich, R. (2004) Biological control through regulated transcriptional coactivators. *Cell* **119**, 157–167
- Métivier, R., Penot, G., Carmouche, R. P., Hübner, M. R., Reid, G., Denger, S., Manu, D., Brand, H., Kos, M., Benes, V., and Gannon, F. (2004) Transcriptional complexes engaged by apo-estrogen receptor-alpha isoforms have divergent outcomes. *EMBO J.* **23**, 3653–3666
- O'Malley, B. W. (2007) Coregulators: from whence came these "master genes". *Mol. Endocrinol.* **21**, 1009–1013
- McKenna, N. J., Cooney, A. J., DeMayo, F. J., Downes, M., Glass, C. K., Lanz, R. B., Lazar, M. A., Mangelsdorf, D. J., Moore, D. D., Qin, J., Steffen, D. L., Tsai, M. J., Tsai, S. Y., Yu, R., Margolis, R. N., Evans, R. M., and O'Malley, B. W. (2009) Minireview: evolution of NURSA, the Nuclear Receptor Signaling Atlas. *Mol. Endocrinol.* **23**, 740–746
- Voss, T. C., Demarco, I. A., Booker, C. F., and Day, R. N. (2005) Corepressor subnuclear organization is regulated by estrogen receptor via a mechanism that requires the DNA-binding domain. *Mol. Cell. Endocrinol.* **231**, 33–47
- Lahusen, T., Henke, R. T., Kagan, B. L., Wellstein, A., and Riegel, A. T. (2009) The role and regulation of the nuclear receptor co-activator AIB1 in breast cancer. *Breast Cancer Res. Treat.* **116**, 225–237
- Spears, M., and Bartlett, J. (2009) The potential role of estrogen receptors and the SRC family as targets for the treatment of breast cancer. *Expert Opin. Ther. Targets* **13**, 665–674
- Shiau, A. K., Barstad, D., Loria, P. M., Cheng, L., Kushner, P. J., Agard, D. A., and Greene, G. L. (1998) The structural basis of estrogen receptor/coactivator recognition and the antagonism of this interaction by tamoxifen. *Cell* **95**, 927–937
- Ellmann, S., Sticht, H., Thiel, F., Beckmann, M. W., Strick, R., and Strissel, P. L. (2009) Estrogen and progesterone receptors: from molecular structures to clinical targets. *Cell. Mol. Life Sci.* **66**, 2405–2426
- Ma, C. X., Sanchez, C. G., and Ellis, M. J. (2009) Predicting endocrine therapy responsiveness in breast cancer. *Oncology* **23**, 133–142
- Wu, Y. L., Yang, X., Ren, Z., McDonnell, D. P., Norris, J. D., Willson, T. M., and Greene, G. L. (2005) Structural basis for an unexpected mode of SERM-mediated ER antagonism. *Mol. Cell* **18**, 413–424
- Delmas, P. D., Bjarnason, N. H., Mitlak, B. H., Ravoux, A. C., Shah, A. S., Huster, W. J., Draper, M., and Christiansen, C. (1997) Effects of raloxifene on bone mineral density, serum cholesterol concentrations, and uterine endometrium in postmenopausal women. *N. Engl. J. Med.* **337**, 1641–1647
- Barrett-Connor, E., Mosca, L., Collins, P., Geiger, M. J., Grady, D., Kornitzer, M., McNabb, M. A., and Wenger, N. K. (2006) Effects of raloxifene on cardiovascular events and breast cancer in postmenopausal women. *N. Engl. J. Med.* **355**, 125–137
- Cimino, D., Fuso, L., Stiglioi, C., Biglia, N., Ponzzone, R., Maggiorotto, F., Russo, G., Cicatiello, L., Weisz, A., Taverna, D., Sismondi, P., and De Bortoli, M. (2008) Identification of new genes associated with breast cancer progression by gene expression analysis of predefined sets of neoplastic tissues. *Int. J. Cancer* **123**, 1327–1338
- Mutarelli, M., Cicatiello, L., Ferraro, L., Grober, O. M., Ravo, M., Facchiano, A. M., Angelini, C., and Weisz, A. (2008) Time-course analysis of genome-wide gene expression data from hormone-responsive human breast cancer cells. *BMC Bioinformatics* **9**, Suppl. 2, S12
- Scafoglio, C., Ambrosino, C., Cicatiello, L., Altucci, L., Ardovino, M., Bon-tempo, P., Medici, N., Molinari, A. M., Nebbioso, A., Facchiano, A., Calogero, R. A., Elkon, R., Menini, N., Ponzzone, R., Biglia, N., Sismondi, P., De Bortoli, M., and Weisz, A. (2006) Comparative gene expression profiling reveals partially overlapping but distinct genomic actions of different antiestrogens in human breast cancer cells. *J. Cell. Biochem.* **98**, 1163–1184
- Ou, K., Kesuma, D., Ganesan, K., Yu, K., Soon, S. Y., Lee, S. Y., Goh, X. P., Hooi, M., Chen, W., Jikuya, H., Ichikawa, T., Kuyama, H., Matsuo, E.,

- Nishimura, O., and Tan, P. (2006) Quantitative profiling of drug-associated proteomic alterations by combined 2-nitrobenzenesulfonyl chloride (NBS) isotope labeling and 2DE/MS identification. *J. Proteome Res.* **5**, 2194–2206
32. Ou, K., Yu, K., Kesuma, D., Hooi, M., Huang, N., Chen, W., Lee, S. Y., Goh, X. P., Tan, L. K., Liu, J., Soon, S. Y., Bin Abdul Rashid, S., Putti, T. C., Jikuya, H., Ichikawa, T., Nishimura, O., Salto-Tellez, M., and Tan, P. (2008) Novel breast cancer biomarkers identified by integrative proteomic and gene expression mapping. *J. Proteome Res.* **7**, 1518–1528
  33. Zheng, B., Han, M., Bernier, M., and Wen, J. K. (2009) Nuclear actin and actin-binding proteins in the regulation of transcription and gene expression. *FEBS J.* **276**, 2669–2685
  34. Gieni, R. S., and Hendzel, M. J. (2009) Actin dynamics and functions in the interphase nucleus: moving toward an understanding of nuclear polymeric actin. *Biochem. Cell Biol.* **87**, 283–306
  35. Hofmann, W. A., Vargas, G. M., Ramchandran, R., Stojiljkovic, L., Goodrich, J. A., and de Lanerolle, P. (2006) Nuclear myosin I is necessary for the formation of the first phosphodiester bond during transcription initiation by RNA polymerase II. *J. Cell. Biochem.* **99**, 1001–1009
  36. Louvet, E., and Percipalle, P. (2009) Transcriptional control of gene expression by actin and myosin. *Int. Rev. Cell Mol. Biol.* **272**, 107–147
  37. Ondrej, V., Lukášová, E., Krejčí, J., Matula, P., and Kozubek, S. (2008) Lamin A/C and polymeric actin in genome organization. *Mol. Cells* **26**, 356–361
  38. Balaguer, P., François, F., Comunale, F., Fenet, H., Boussioux, A. M., Pons, M., Nicolas, J. C., and Casellas, C. (1999) Reporter cell lines to study the estrogenic effects of xenoestrogens. *Sci. Total Environ.* **233**, 47–56
  39. Pacilio, C., Germano, D., Addeo, R., Altucci, L., Petrizzi, V. B., Cancemi, M., Cicatiello, L., Salzano, S., Lallemand, F., Michalides, R. J., Bresciani, F., and Weisz, A. (1998) Constitutive overexpression of cyclin D1 does not prevent inhibition of hormone-responsive human breast cancer cell growth by antiestrogens. *Cancer Res.* **58**, 871–876
  40. Sotiropoulos, A., Gineitis, D., Copeland, J., and Treisman, R. (1999) Signal-regulated activation of serum response factor is mediated by changes in actin dynamics. *Cell* **98**, 159–169
  41. Cicatiello, L., Addeo, R., Sasso, A., Altucci, L., Petrizzi, V. B., Borgo, R., Cancemi, M., Caporali, S., Caristi, S., Scafoglio, C., Teti, D., Bresciani, F., Perillo, B., and Weisz, A. (2004) Estrogens and progesterone promote persistent CCND1 gene activation during G1 by inducing transcriptional derepression via c-Jun/c-Fos/estrogen receptor (progesterone receptor) complex assembly to a distal regulatory element and recruitment of cyclin D1 to its own gene promoter. *Mol. Cell. Biol.* **24**, 7260–7274
  42. Chaurasia, G., Malhotra, S., Russ, J., Schnoegl, S., Hänig, C., Wanker, E. E., and Futschik, M. E. (2009) UniHI 4: new tools for query, analysis and visualization of the human protein-protein interactome. *Nucleic Acids Res.* **37**, D657–D660
  43. Giretti, M. S., Fu, X. D., De Rosa, G., Sarotto, I., Baldacci, C., Garibaldi, S., Mannella, P., Biglia, N., Sisonidi, P., Genazzani, A. R., and Simoncini, T. (2008) Extra-nuclear signalling of estrogen receptor to breast cancer cytoskeletal remodelling, migration and invasion. *PLoS One* **3**, e2238
  44. Hartwig, J. H., Thelen, M., Rosen, A., Janmey, P. A., Nairn, A. C., and Aderem, A. (1992) MARCKS is an actin filament crosslinking protein regulated by protein kinase C and calcium-calmodulin. *Nature* **356**, 618–622
  45. Rigaut, G., Shevchenko, A., Rutz, B., Wilm, M., Mann, M., and Séraphin, B. (1999) A generic protein purification method for protein complex characterization and proteome exploration. *Nat. Biotechnol.* **17**, 1030–1032
  46. Endoh, H., Maruyama, K., Masuhiro, Y., Kobayashi, Y., Goto, M., Tai, H., Yanagisawa, J., Metzger, D., Hashimoto, S., and Kato, S. (1999) Purification and identification of p68 RNA helicase acting as a transcriptional coactivator specific for the activation function 1 of human estrogen receptor alpha. *Mol. Cell. Biol.* **19**, 5363–5372
  47. Ogawa, S., Oishi, H., Mezaki, Y., Kouzu-Fujita, M., Matsuyama, R., Nakagomi, M., Mori, E., Murayama, E., Nagasawa, H., Kitagawa, H., Yanagisawa, J., Yano, T., and Kato, S. (2005) Repressive domain of unliganded human estrogen receptor alpha associates with Hsc70. *Genes Cells* **10**, 1095–1102
  48. Grummt, I. (2006) Actin and myosin as transcription factors. *Curr. Opin. Genet. Dev.* **16**, 191–196
  49. Hofmann, W. A., Stojiljkovic, L., Fuchsova, B., Vargas, G. M., Mavrommatis, E., Philimonenko, V., Kyselá, K., Goodrich, J. A., Lessard, J. L., Hope, T. J., Hozak, P., and de Lanerolle, P. (2004) Actin is part of pre-initiation complexes and is necessary for transcription by RNA polymerase II. *Nat. Cell Biol.* **6**, 1094–1101
  50. Cheng, P. C., Chang, H. K., and Chen, S. H. (2010) Quantitative nano-proteomics for protein complexes (QNanoPX) related to estrogen transcriptional action. *Mol. Cell. Proteomics* **9**, 209–224
  51. Lee, Y. H., Campbell, H. D., and Stallcup, M. R. (2004) Developmentally essential protein flightless I is a nuclear receptor coactivator with actin binding activity. *Mol. Cell. Biol.* **24**, 2103–2117
  52. Archer, S. K., Behm, C. A., Claudianos, C., and Campbell, H. D. (2004) The flightless I protein and the gelsolin family in nuclear hormone receptor-mediated signalling. *Biochem. Soc. Trans.* **32**, 940–942
  53. Kojetin, D. J., Burris, T. P., Jensen, E. V., and Khan, S. A. (2008) Implications of the binding of tamoxifen to the coactivator recognition site of the estrogen receptor. *Endocr. Relat. Cancer* **15**, 851–870
  54. Shiau, A. K., Barstad, D., Radek, J. T., Meyers, M. J., Nettles, K. W., Katzenellenbogen, B. S., Katzenellenbogen, J. A., Agard, D. A., and Greene, G. L. (2002) Structural characterization of a subtype-selective ligand reveals a novel mode of estrogen receptor antagonism. *Nat. Struct. Biol.* **9**, 359–364
  55. Zhu, X., Zeng, X., Huang, B., and Hao, S. (2004) Actin is closely associated with RNA polymerase II and involved in activation of gene transcription. *Biochem. Biophys. Res. Commun.* **321**, 623–630
  56. Sampath, P., and Pollard, T. D. (1991) Effects of cytochalasin, phalloidin, and pH on the elongation of actin filaments. *Biochemistry* **30**, 1973–1980
  57. Kukalev, A., Nord, Y., Palmberg, C., Bergman, T., and Percipalle, P. (2005) Actin and hnRNP U cooperate for productive transcription by RNA polymerase II. *Nat. Struct. Mol. Biol.* **12**, 238–244
  58. Hofmann, W. A. (2009) Cell and molecular biology of nuclear actin. *Int. Rev. Cell Mol. Biol.* **273**, 219–263
  59. Kyselá, K., Philimonenko, A. A., Philimonenko, V. V., Janáček, J., Kahle, M., and Hozák, P. (2005) Nuclear distribution of actin and myosin I depends on transcriptional activity of the cell. *Histochem. Cell Biol.* **124**, 347–358
  60. Wilson, D. N., and Nierhaus, K. H. (2005) Ribosomal proteins in the spotlight. *Crit. Rev. Biochem. Mol. Biol.* **40**, 243–267
  61. Tokunaga, K., Shibuya, T., Ishihama, Y., Tadakuma, H., Ide, M., Yoshida, M., Funatsu, T., Ohshima, Y., and Tani, T. (2006) Nucleocytoplasmic transport of fluorescent mRNA in living mammalian cells: nuclear mRNA export is coupled to ongoing gene transcription. *Genes Cells* **11**, 305–317
  62. Brogna, S., Sato, T. A., and Rosbash, M. (2002) Ribosome components are associated with sites of transcription. *Mol. Cell* **10**, 93–104
  63. McKenna, N. J., and O'Malley, B. W. (2002) Minireview: nuclear receptor coactivators—an update. *Endocrinology* **143**, 2461–2465
  64. Cicatiello, L., Mutarelli M., Grober, O. M., Paris, O., Ferraro, L., Ravo, M., Tarallo, R., Luo, S., Schroth, G. P., Seifert, M., Zinser, C., Chiusano, M. L., Traini, A., De Bortoli, M., and Weisz, A. (2010) Estrogen receptor alpha controls a gene network in luminal-like breast cancer cells comprising multiple transcription factors and microRNAs. *Am. J. Pathol.*, in press
  65. Belandia, B., and Parker, M. G. (2003) Nuclear receptors: a rendezvous for chromatin remodeling factors. *Cell* **114**, 277–280
  66. Sabbah, M., Kang, K. I., Tora, L., and Redeuilh, G. (1998) Oestrogen receptor facilitates the formation of preinitiation complex assembly: involvement of the general transcription factor TFIIB. *Biochem. J.* **336**, 639–646
  67. Wu, S. Y., Thomas, M. C., Hou, S. Y., Likhite, V., and Chiang, C. M. (1999) Isolation of mouse TFIID and functional characterization of TBP and TFIID in mediating estrogen receptor and chromatin transcription. *J. Biol. Chem.* **274**, 23480–23490
  68. Lonard, D. M., Nawaz, Z., Smith, C. L., and O'Malley, B. W. (2000) The 26S proteasome is required for estrogen receptor-alpha and coactivator turnover and for efficient estrogen receptor-alpha transactivation. *Mol. Cell* **5**, 939–948
  69. Reid, G., Hübner, M. R., Métivier, R., Brand, H., Denger, S., Manu, D., Beaudouin, J., Ellenberg, J., and Gannon, F. (2003) Cyclic, proteasome-mediated turnover of unliganded and liganded ERalpha on responsive promoters is an integral feature of estrogen signaling. *Mol. Cell* **11**, 695–707
  70. Métivier, R., Penot, G., Hübner, M. R., Reid, G., Brand, H., Kos, M., and Gannon, F. (2003) Estrogen receptor-alpha directs ordered, cyclical, and

- combinatorial recruitment of cofactors on a natural target promoter. *Cell* **115**, 751–763
71. Percipalle, P. (2009) The long journey of actin and actin-associated proteins from genes to polysomes. *Cell. Mol. Life Sci.* **66**, 2151–2165
72. Métivier, R., Huet, G., Gallais, R., Finot, L., Petit, F., Tiffocche, C., Mérot, Y., LePéron, C., Reid, G., Penot, G., Demay, F., Gannon, F., Flouriot, G., and Salbert, G. (2008) Dynamics of estrogen receptor-mediated transcriptional activation of responsive genes in vivo: apprehending transcription in four dimensions. *Adv. Exp. Med. Biol.* **617**, 129–138
73. Chen, M., and Shen, X. (2007) Nuclear actin and actin-related proteins in chromatin dynamics. *Curr. Opin. Cell Biol.* **19**, 326–330
74. Andrin, C., and Hendzel, M. J. (2004) F-actin-dependent insolubility of chromatin-modifying components. *J. Biol. Chem.* **279**, 25017–25023
75. Zhao, K., Wang, W., Rando, O. J., Xue, Y., Swiderek, K., Kuo, A., and Crabtree, G. R. (1998) Rapid and phosphoinositid-dependent binding of the SWI/SNF-like BAF complex to chromatin after T lymphocyte receptor signaling. *Cell* **95**, 625–636
76. Fréhlick, L. J., Eirín-López, J. M., and Ausió, J. (2007) New insights into the nucleophosmin/nucleoplasmin family of nuclear chaperones. *BioEssays* **29**, 49–59
77. Lindström, M. S. (2009) Emerging functions of ribosomal proteins in gene-specific transcription and translation. *Biochem. Biophys. Res. Commun.* **379**, 167–170
78. Berghöfer-Hochheimer, Y., Zurek, C., Wölfl, S., Hemmerich, P., and Munder, T. (1998) L7 protein is a coregulator of vitamin D receptor-retinoid X receptor-mediated transactivation. *J. Cell. Biochem.* **69**, 1–12
79. Whelley, S. M. (1985) Regulation of uterine nucleolar RNA synthesis by estrogens. *Biol. Reprod.* **33**, 1–10
80. Whelley, S. M. (1986) Estradiol regulation of uterine nucleolar estradiol binding sites. *Biochim. Biophys. Acta* **880**, 179–188
81. Sebastian, T., and Thampan, R. V. (2002) Nuclear estrogen receptor II (nER-II) is involved in estrogen-dependent ribonucleoprotein transport in the goat uterus: II. isolation and characterization of three small nuclear ribonucleoprotein proteins which bind to nER-II. *J. Cell. Biochem.* **84**, 227–236
82. Solakidi, S., Psarra, A. M., and Sekeris, C. E. (2005) Differential subcellular distribution of estrogen receptor isoforms: localization of ER $\alpha$  in the nucleoli and ER $\beta$  in the mitochondria of human osteosarcoma SaOS-2 and hepatocarcinoma HepG2 cell lines. *Biochim. Biophys. Acta* **1745**, 382–392
83. Taddei, A. (2007) Active genes at the nuclear pore complex. *Curr. Opin. Cell Biol.* **19**, 305–310
84. Warner, J. R., and McIntosh, K. B. (2009) How common are extraribosomal functions of ribosomal proteins? *Mol Cell.* **34**, 3–11